EFECTES DELS INHIBIDORS DE LA CICLOOXIGENASA EN CÈL·LULES HEPÀTIQUES I EL SEU PAPER EN LA INFLAMACIÓ I FIBROSI HEPÀTICA EXPERIMENTAL

Anna Planagumà Ferrer

Resultats

4 RESULTATS

ARTICLE 1

L'aspirina (ASA) regula l'activitat de la 5-lipooxigenasa i del receptor activat per proliferadors de peroxisomes α –mediador de l'alliberament de CINC-1 en cèl·lules hepàtiques de rata: accions innovadores de la lipoxina A_4 (LXA_4) i de la 15-epi-LXA_4 derivada de l'acció de l'ASA.

1. L'ASA produeix el redireccionament del metabolisme de l'àcid araquidònic de la biosíntesi de PGE_2 cap a la biosíntesi de LTB_4 i 15-epi-LXA_4 en cèl·lules de Kupffer.

El fetge és el primer òrgan que rep tot el volum d'ASA absorbit per l'intestí i juga un paper important en la hidròlisi de l'àcid acetilsalicílic a salicilat. Per aquest motiu, les cèl·lules hepàtiques són probablement el tipus cel·lular que majoritàriament es troba amb el component actiu de l'ASA. En concret vam centrar el nostre estudi en les cèl·lules de Kupffer perquè aquests macròfags residents del fetge expressen el mRNA de la COX-1, la COX-2, la 5-LO i la FLAP i constitueixen la font més important d'eicosanoids en el sinusoide hepàtic. Es va observar que en les cèl·lules de Kupffer l'efecte inhibidor de l'ASA sobre els productes derivats de la COX (p. ex. la PGE_2) estava associat amb un increment dosi depenent del producte de la 5-LO, el LTB_4, i de l'eicosanoid antiinflamatori, la 15-epi-LXA_4. L'ASA també estimula de manera dosi depenent l'activitat de la 5-LO i la producció de LTB_4 en la línia cel·lular de macròfags de rata CRL-2192. En conjunt aquests resultats concorden amb l'evidència que tot i que l'efecte primari de l'ASA sigui la inhibició de la COX amb una conseqüent reducció de la formació de PGs, aquest AINE també exerceix efectes significatius en altres vies del metabolisme de l'AA (p. ex. en la biosíntesi de LTB_4 i 15-epi-LXA_4).

2. L'ASA modula el PPARα en hepatòcits de rata.

Per estudiar la significació biològica de les accions de l'ASA en els macròfags de rata, vam centrar els nostres estudis en el context del sinusoide hepàtic a on trobem les KCs en contacte directe amb els hepatòcits. Vam dirigir els experiments cap a l'estudi de la influència de l'ASA i de productes derivats de l'AA sobre els factors de transcripció gènica implicats en el control de

la inflamació en les KCs. En concret vam focalitzar el nostre interès en un grup d'aquests factors transcripcionals, la família dels PPARs, i específicament en el PPARα, la isoforma predominant en hepatòcits. L'ASA redueix significativament els nivells de PPARα en hepatòcits de rata. El producte derivat de la 5-LO, el LTB_4, la 15-epi-LXA_4 i l'agonista selectiu del PPARα, l'activador Wy-14643, disminueixen l'expressió de la proteïna del PPARα en hepatòcits de rata. L'observació que l'ASA disminuïa l'expressió de la proteïna del PPARα va ser confirmada posteriroment en extractes nuclears de la línia cel·lular de leucòcits mononuclears humans (cèl·lules THP-1) indicant que aquesta propietat de l'ASA no es restringeix només al fetge. Contràriament la PGE_2 tant sola com en combinació amb LTB_4 no indueix cap canvi en l'expressió de la proteïna del PPARα. De la mateixa manera els nivells de PPARα en hepatòcits de rata en cultiu no es van veure modificats pels inhibidors selectius de COX-1 i COX-2, el SC-560 i celecoxib respectivament.

3. L'ASA modula la secreció de la citoquina quimioatraient induïda per neutròfils-1 (CINC-1) en hepatòcits de rata.

Degut a que els reguladors transcripcionals de la família dels PPARs estan involucrats en la modulació de diferents gens inflamatoris, incloent els membres de la família de la interleuquina-8 (IL-8), vam avaluar els efectes de l'ASA sobre la secreció de CINC-1 (l'equivalent de rata a la IL-8 humana i/o el producte gènic de regulació del creixement α (GROα)) en hepatòcits de rata. Les incubacions d'hepatòcits de rata en cultiu amb ASA van produir una disminució dels nivells de CINC-1. El mecanisme pel qual l'ASA disminueix la secreció de CINC-1 és desconegut, tot i que l'agonista selectiu del PPARα, l'activador Wy-14643, redueix la producció de CINC-1 en hepatòcits de rata, implicant una acció de l'ASA a nivell de PPARα. Pel contrari, l'addició de LTB_4 en associació amb PGE_2 incrementa significativament la secreció de CINC-1 en hepatòcits de rata.

4. La LXA_4 i la 15-epi-LXA_4 derivada de l'acció de l'ASA modulen l'activitat de la 5-LO, l'expressió de la proteïna del PPARα i l'alliberament de CINC-1.

La LXA_4, un eicosanoid endogen que està associat a senyals antiinflamatòries i que és generat per la via biosintètica que implica la lipoxigenació dual de l'AA per part de la 5- i la 15-LO o la 5- i la 12-LO, inhibeix significativament l'activitat de la 5-LO en macròfags. La PGE_2 sola o en combinació amb la LXA_4 disminueix significativament l'activitat de la 5-LO en macròfags.

Recentment s'ha vist en neutròfils que la PGE_2 indueix el canvi en la biosíntesi d'eicosanoids de la via predominant de la síntesi de LTB_4 a la via de la síntesi de LXA_4. Els nostres resultats demostren que en macròfags de rata la LXA_4 inhibeix l'activitat de la 5-LO d'una manera semblant a la PGE_2 suggerint que aquest eicosanoid antiinflamatori endogen juga un paper actiu en el canvi de formació dels diferents tipus d'eicosanoids possiblement durant la fase de resolució de la inflamació. Per altra banda, la 15-epi-LXA_4 derivada de l'ASA, un mediador lipídic endogen que mimetitza l'acció de la LXA_4 nativa, significativament redueix els nivells de PPARα i CINC-1 en hepatòcits. En resum, i perquè l'activitat de la 5-LO i els nivells de PPARα i CINC-1 estan involucrats en l'extensió i la duració de la resposta inflamatòria, aquests resultats proporcionen mecanismes moleculars addicionals a aquestes senyals endògenes que proporcionen una aturada del procés inflamatori.

Aspirin (ASA) regulates 5-lipoxygenase activity and peroxisome proliferator-activated receptor α-mediated CINC-1 release in rat liver cells: novel actions of lipoxin A_4 (LXA_4) and ASA-triggered 15-epi-LXA_4 [1]

ANNA PLANAGUMÀ, ESTHER TITOS, MARTA LÓPEZ-PARRA, JOAN GAYA,* GLORIA PUEYO,‡ VICENTE ARROYO,† AND JOAN CLÀRIA[2]

DNA Unit, *Hormonal Laboratory and †Liver Unit, Hospital Clínic, Institut d'Investigacions Biomèdiques August Pi i Sunyer (IDIBAPS), Universitat de Barcelona; and ‡Química Farmacéutica Bayer S.A. (C.C. Division), Barcelona 08036, Spain

SPECIFIC AIM

The aim of this study was to explore new mechanisms of action of aspirin (ASA) other than cyclooxygenase (COX) and prostaglandin (PG) inhibition that may contribute to its anti-inflammatory and antithrombotic properties. We assessed the effects of ASA on eicosanoid-generating pathways and its effect on peroxisome proliferator-activated receptor α (PPARα) and cytokine-induced neutrophil chemoattractant-1 (CINC-1) levels in rat liver cells.

PRINCIPAL FINDINGS

1. ASA switches arachidonic acid metabolism from PGE_2 to leukotriene B_4 (LTB_4) and 15-epi-lipoxin A_4 (15-epi-LXA_4) biosynthesis in rat Kupffer cells

The liver is the first organ to receive the bulk of absorbed ASA from the gut and plays a major role in the hydrolysis of acetylsalicylic acid to salicylate. For this reason, hepatic cells are probably the cell types that encounter most of ASA's active compound. We focused our interest in Kupffer cells because these liver resident macrophages express COX-1, COX-2, 5-LO, and 5-LO-activating protein (FLAP) mRNA (**Fig. 1*A***) and constitute the most important source of eicosanoids within the liver sinusoid. In Kupffer cells, we found that the inhibitory effect of ASA on COX-derived products (e.g., PGE_2) was associated with a dose-dependent increase of the 5-LO product LTB_4 and the endogenous anti-inflammatory eicosanoid 15-epi-LXA_4 (Fig. 1*B*). ASA also dose-dependently stimulated 5-LO activity and LTB_4 production in rat CRL-2192 macrophages. Together, these findings are consistent with the notion that although the primary effect of ASA is the inhibition of COX with a consequent reduction of PG formation, this nonsteroidal anti-inflammatory drug (NSAID) exerts significant effects on other pathways for arachidonic acid metabolism (i.e., LTB_4 and 15-epi-LXA_4 biosynthesis).

2. ASA modulates peroxisome proliferator-activated receptor α (PPARα) in rat hepatocytes

To ascertain the biological significance of ASA actions in rat macrophages, we put our findings into the context of the liver sinusoid where Kupffer cells are in close contact with hepatocytes. We wanted to examine the influence of ASA and Kupffer cell-derived arachidonic acid products on gene transcriptional factors implicated in the control of inflammation. We focused our investigation on one group of such transcriptional factors—the PPAR family—and specifically in PPARα, the predominant PPAR subtype in hepatocytes. As shown in **Fig. 2*A***, ASA significantly reduced PPARα levels in rat hepatocytes. The 5-LO-derived product LTB_4, a member of the novel class of ASA-triggered 15*R* containing LX (15-epi-LXA_4), and the selective PPARα agonist activator Wy-14643 decreased PPARα protein expression in rat hepatocytes (Fig. 2*A*). The observation that ASA decreases PPARα protein expression in rat hepatocytes was further confirmed in nuclear extracts from a human mononuclear leukocyte cell line (THP-1 cells) (Fig. 2*B*), indicating that this ASA property is not restricted to the liver scenario. Conversely and as shown in Fig. 2*C*, PGE_2 alone and PGE_2 in association with LTB_4 did not induce any change in PPARα protein expression. Similarly, PPARα levels in

[1] To read the full text of this article, go to http://www.fasebj.org/cgi/doi/10.1096/fj.02–0224fje; to cite this article, use *FASEB J.* (October 4, 2002) 10.1096/fj.02–0224fje

[2] Correspondence: DNA Unit, Hospital Clinic, Villarroel 170, Barcelona 08036, Spain. E-mail: jclaria@clinic.ub.es

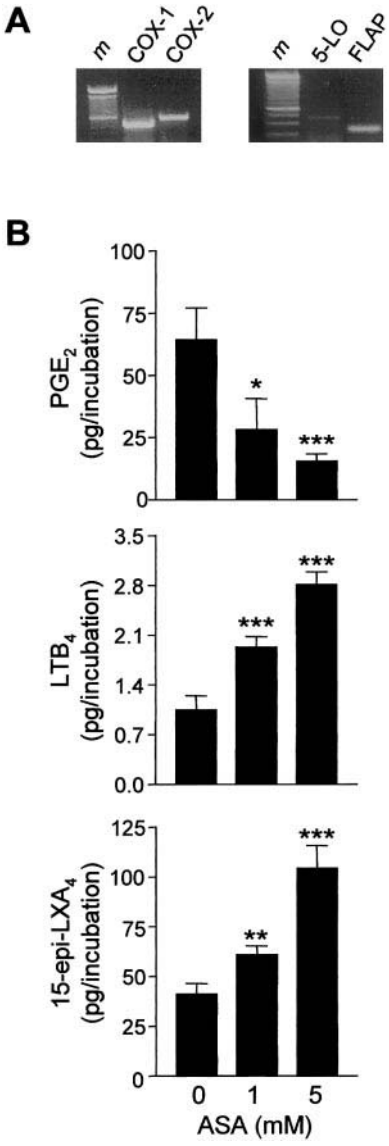

Figure 1. *A)* Detection of COX-1, COX-2, 5-LO, and FLAP mRNA expression by RT-PCR in rat Kupffer cells. *m*, molecular weight DNA ladder. *B)* Effect of ASA on PGE_2, LTB_4 and 15-epi-LXA_4 biosynthesis in rat Kupffer cells. Results represent the mean ± SE of 11 different experiments. $*P < 0.05$, $**P < 0.025$, and $***P < 0.005$ vs. vehicle.

rat hepatocyte cultures were not modified by the selective COX-1 and COX-2 inhibitors SC-560 and celecoxib, respectively (Fig. 2*C*).

3. ASA modulates the secretion of cytokine-induced neutrophil chemoattractant-1 (CINC-1) by rat hepatocytes

Because the PPAR family of transcriptional regulators is involved in the modulation of various inflammatory genes, including members of the interleukin-8 (IL-8) family, we next evaluated the effects of ASA on the secretion of CINC-1 [the rat counterpart of human IL-8 and/or growth-regulated gene product α (GROα)] by rat hepatocytes. Incubation of rat hepatocyte cultures with ASA resulted in decreased levels of CINC-1. The mechanism by which ASA down-regulates CINC-1 secretion is unknown, although the selective PPARα agonist activator Wy-14643 reduced CINC-1 production in rat hepatocytes, implying an action of ASA at the level of PPARα. In contrast, addition of LTB_4 in association with PGE_2 significantly increased CINC-1 secretion by rat hepatocytes.

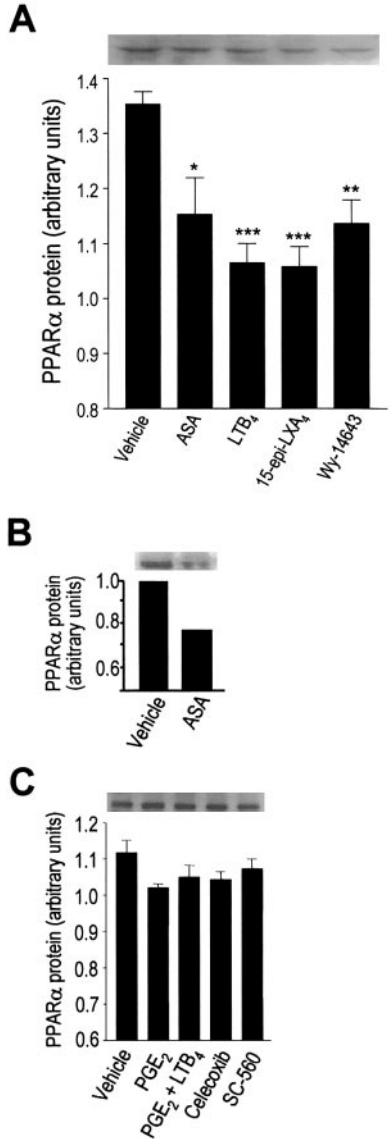

Figure 2. Effect of ASA and Kupffer cell-derived arachidonic acid metabolites on PPARα protein expression. *A)* Rat hepatocytes were exposed to either vehicle (0.1% ethanol), 1 mM ASA, 1 μM LTB_4, 1 μM 15-epi-LXA_4-methyl ester, or 0.1 μM Wy-14643 for 24 h at 37°C and nuclear extracts were probed with a specific anti-murine PPARα antiserum. *B)* Human mononuclear leukocytes (THP-1 cells) were exposed to vehicle (0.1% ethanol) or 1 mM ASA for 24 h at 37°C and nuclear extracts analyzed by Western blot. *C)* Rat hepatocytes were exposed to either vehicle (0.1% ethanol), 0.3 μM PGE_2, 0.3 μM PGE_2 in association with 1 μM LTB_4, 3 μM celecoxib, or 3 μM SC-560 for 24 h at 37°C and nuclear extracts were probed as described above. Results are representative of 12 separate experiments. $*P < 0.05$, $**P < 0.005$, and $***P < 0.001$ vs. vehicle.

4. LXA_4 and ASA-triggered 15-epi-LXA_4 modulate 5-LO activity, PPARα protein expression and CINC-1 release

LXA_4, an endogenous eicosanoid that carries "stop signals" for inflammation and is generated via biosynthetic pathways that involve the dual lipoxygenation of arachidonic acid by either 5- and 15-LO or 5- and 12-LO, significantly inhibited 5-LO activity in rat macrophages. PGE_2 alone and PGE_2 in association with LXA_4 significantly decreased macrophage 5-LO activity. It was recently reported in human neutrophils that PGE_2 induces a switch in eicosanoid biosynthesis from the predominantly LTB_4- and 5-LO-initiated pathway to LXA_4. Our findings demonstrating that in rat macrophages LXA_4 inhibits 5-LO activity to a similar extent as PGE_2 suggest that this endogenous anti-inflammatory eicosanoid plays an active role in the switching of eicosanoid classes possibly during resolution of inflammation. On the other hand, ASA-triggered 15-epi-LXA_4, an endogenous lipid-derived mediator that mimics the action of native LXA_4, significantly reduced PPARα and CINC-1 levels in hepatocytes. Taken together and because 5-LO activity and PPARα and CINC-1 levels are involved in the extent and duration of the inflammatory response, these findings provide additional molecular mechanisms for these putative endogenous stop signals of inflammation.

CONCLUSIONS AND SIGNIFICANCE

ASA is an NSAID used to treat a wide variety of medical conditions. Besides to its well-known anti-inflammatory, analgesic, and anti-pyretic properties, ASA inhibits platelet aggregation, is useful in preventing myocardial infarction and stroke, has neuroprotective actions, and decreases the incidence of cancer. Although most pharmacological properties of ASA are related to its ability to acetylate COX leading to irreversible inhibition of PG synthesis, the complete mechanism of action of ASA is still a subject of debate. At high doses, for instance, some properties of ASA are not mediated by inhibition of COX and PGs. ASA is able to modulate activity of the nuclear factor-κB, activator protein 1, the heat shock transcriptional factor, and the p38 and p44Erk1 and p42Erk2 mitogen-activated protein kinases. In the current study, we provide new molecular mechanisms underlying the pleiotropic response to ASA by demonstrating that this NSAID promotes the formation of endogenous anti-inflammatory compounds (e.g., 15-epi-LXA_4) and modulates 5-LO activity and PPARα and CINC-1 levels in rat liver sinusoidal cells.

A hypothetical scheme for the actions of ASA on arachidonic acid metabolism in rat liver cells is illustrated in **Fig. 3**. In Kupffer cells, ASA inhibits COX and PGE_2 biosynthesis and favors the oxidation of arachidonic acid via the 5-LO pathway (e.g., LTB_4). The increase in LTB_4 formation after ASA treatment may be

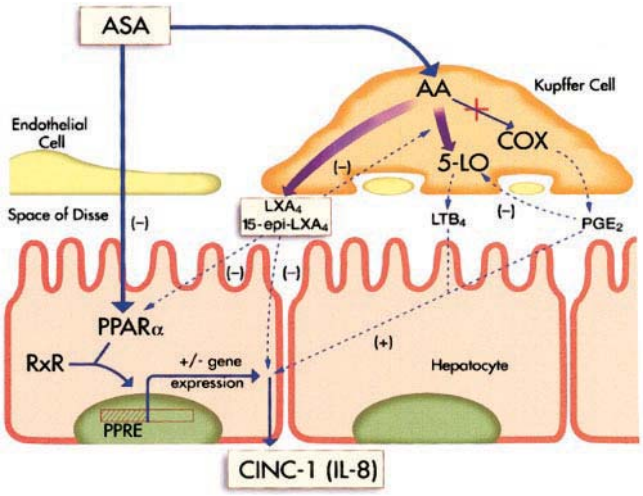

Figure 3. Hypothetical scheme of ASA actions in rat liver sinusoidal cells.

secondary to either the shunting of arachidonic acid to the 5-LO pathway or abolishment of the inhibitory action exerted by COX-derived products (including PGE_2) on LTB_4 biosynthesis. Before ASA is extensively hydrolyzed to salicylate in the liver and enters systemic circulation, this NSAID triggers the release of potent biologically active eicosanoids (i.e.,15-epi-LXA_4) by Kupffer cells. Since Kupffer cells have COX-2 and 5-LO in place, the formation of ASA-triggered 15-epi-LXA_4 in these liver resident macrophages may occur by interaction of ASA-acetylated COX-2 with 5-LO or conversion via transcellular routes of 15*R*-HETE released by underlying hepatocytes. Unlike endothelial and epithelial cells, the biosynthesis of 15*R*-HETE in hepatocytes is initiated by COX-2-independent pathways. Regardless of their cellular origin, liver cells are a rich source of 15-epi-LXA_4 during ASA treatment. These ASA-triggered 15-epi-LXA_4 may exert diverse anti-inflammatory activities in autocrine and paracrine fashion, contributing to the broad range of beneficial actions of ASA. In the current investigation, we demonstrate that besides decreasing 5-LO activity in macrophages (to an extent similar to PGE_2), ASA-triggered 15-epi-LXA_4 significantly inhibit PPARα and CINC-1 levels in underlying hepatocytes. In rat hepatocytes, ASA directly reduces PPARα protein levels and the secretion of CINC-1 (Fig. 3). In contrast, LTB_4 together with PGE_2 generated in Kupffer cells stimulates CINC-1 production in adjacent hepatocytes.

Because arachidonic acid-derived products along with gene transcriptional regulators such as PPARα and target genes such as CINC-1 play a central role in the control of inflammation, our findings provide an important contribution to understanding the mechanism of action of one of the most widely used NSAIDs: ASA. The link between membrane-derived bioactive lipids such as LXA_4 and ASA-triggered 15-epi-LXA_4 and the modulation of 5-LO, PPARα, and CINC-1 provides new opportunities for investigations into cell signaling and new targets for drug design. FJ

The FASEB Journal express article 10.1096/fj.02-0224fje. Published online October 4, 2002.

Aspirin (ASA) regulates 5-lipoxygenase activity and peroxisome proliferator-activated receptor α-mediated CINC-1 release in rat liver cells: novel actions of lipoxin A_4 (LXA_4) and ASA-triggered 15-epi-LXA_4

Anna Planagumà,* Esther Titos,* Marta López-Parra,* Joan Gaya,[†] Gloria Pueyo, [§] Vicente Arroyo, [‡] and Joan Clària*

*DNA Unit, [†]Hormonal Laboratory, and [‡]Liver Unit, Hospital Clínic, Institut d´Investigacions Biomèdiques August Pi i Sunyer (IDIBAPS), Universitat de Barcelona; and [§]Química Farmacéutica Bayer S.A. (C.C. Division), Barcelona 08036, Spain

Corresponding author: Joan Clària, DNA Unit, Hospital Clínic, Villarroel 170, Barcelona 08036, Spain. E-mail: jclaria@clinic.ub.es

ABSTRACT

The mechanism of action of aspirin (ASA) is related to cyclooxygenase (COX) inhibition, but additional actions cannot be excluded for their antiinflammatory properties and antithrombotic activity. In the current investigation, we examined the effects of ASA on COX and 5-lipoxygenase (5-LO) pathways and its impact on peroxisome proliferator-activated receptor α (PPARα) and cytokine-induced neutrophil chemoattractant-1 (CINC-1) levels in rat liver cells. In Kupffer cells, the liver resident macrophages, ASA switched eicosanoid biosynthesis from prostaglandin E_2 (PGE_2) to leukotriene B_4 (LTB_4) and 15-epi-lipoxin A_4 (15-epi-LXA_4) formation. In hepatocytes, ASA significantly inhibited PPARα protein expression and CINC-1 secretion, effects that were also observed in hepatocytes exposed to the selective PPARα agonist Wy-14643. In contrast, treatment of hepatocytes with PGE_2 in association with LTB_4 had no significant effect on PPARα but stimulated CINC-1 release. Interestingly, the endogenous antiinflammatory eicosanoids LXA_4 and ASA-triggered 15-epi-LXA_4, in addition to inhibiting macrophage 5-LO activity to a similar extent as PGE_2, significantly reduced PPARα and CINC-1 levels in hepatocytes. Taken together and because arachidonic acid-derived products, PPARα levels, and CINC-1 secretion are involved in the extent and duration of an inflammatory response, these findings provide additional molecular mechanisms for the pharmacological properties of ASA.

Key words: Kupffer cells • hepatocytes • nonsteroidal antiinflammatory drug • arachidonic acid metabolites

Aspirin (acetylsalicylic acid, ASA) is a nonsteroidal antiinflammatory drug (NSAID) used in the treatment of a wide variety of medical conditions. In addition to the well-known antiinflammatory, analgesic and antipyretic properties, ASA also inhibits platelet aggregation, is useful in preventing myocardial infarction and stroke, has neuroprotective

actions, and decreases the incidence of cancer (1–4). Although most of the pharmacological properties of ASA are related to its ability to acetylate cyclooxygenase (COX), leading to the irreversible inhibition of prostaglandin (PG) synthesis (5), the complete mechanism of action of ASA is still a subject of interest and debate. At high doses, for instance, there are properties of ASA that are independent of COX and PG inhibition. In this regard, many studies have shown that ASA is able to either activate the heat shock transcriptional factor and the p38 mitogen-activated protein kinase (6, 7) or to inhibit the mitogen-activated protein kinases p44Erk1 and p42Erk2 and the activity of transcriptional factors such as nuclear factor-κB and activator protein 1 (8–10). Finally, and of particular interest, ASA triggers the biosynthesis of endogenous antiinflammatory compounds (termed 15-epi-lipoxins, 15-epi-LX), putative endogenous "breaking signals" for leukocyte recruitment that play a key role in the resolution of inflammation (11, 12).

The liver is the first organ to receive the bulk of absorbed ASA from the gut and plays a major role in the hydrolysis of acetylsalicylic acid to salicylate (13, 14). For this reason, hepatic cells are probably the cell types that encounter most of ASA's active compound. In a previous investigation, we assessed the impact of ASA on arachidonic acid metabolism in liver cells and specifically in rat hepatocytes (15). In these parenchymal liver cells, we found that in addition to inhibiting the COX pathway, pharmacological concentrations of ASA favor arachidonic acid metabolism to 15*R*-HETE and to the formation of 15-epi-LXA_4 (15). In the current investigation, we further evaluated the impact of ASA on arachidonic acid metabolism in sinusoidal liver cells by examining the effects of this NSAID on COX and 5-lipoxygenase (5-LO)-initiated pathways in rat Kupffer cells, the liver resident macrophages. Given that eicosanoids are lipid mediators of several important cellular processes, including the regulation of transcription factors involved in the duration and extent of the inflammatory response, we performed additional studies assessing the effects of ASA and arachidonic acid-derived products on peroxisome proliferator-activated receptor α (PPARα) protein expression and cytokine-induced neutrophil chemoattractant-1 (CINC-1) secretion in rat hepatocytes.

MATERIALS AND METHODS

Cell isolation and culture

Male adult Wistar Rats (Charles River, Saint Aubin les Elseuf, France) weighing 200–300 g were anesthetized with ketamine (50 mg/kg body weight), and liver cells were isolated by *in situ* collagenase perfusion through the portal vein according to the method of Berry and Friend with modifications (16, 17). In brief, livers were perfused for 20 min at a flow rate of 14 ml/min at 37°C with Hank's balanced salt solution without calcium and magnesium (HBSS) containing 10 mmol/L HEPES (pH 7.4) and 1 mmol/L EGTA, followed by 5 min with HBSS containing 10 mmol/L HEPES (pH 7.4), 1.3 mmol/L $CaCl_2$, and 0.6% bovine serum albumin (BSA) and then 10 min with a 0.05% collagenase (A type) solution containing 10 mmol/L HEPES (pH 7.4) and 1.3 mmol/L $CaCl_2$. The resultant digested liver was excised and minced, and the dispersed cells were passed through nylon mesh filters (100 μm). The hepatic cell suspension was centrifuged twice at 50*g* for 5 min, and the supernatant containing mainly nonparenchymal cells (i.e., Kupffer, hepatic stellate, and endothelial cells) was used for Kupffer cell isolation as described subsequently. The cell pellet enriched with hepatocytes was washed twice with cold HBSS

containing 10 mmol/L HEPES (pH 7.4), 1.3 mmol/L $CaCl_2$, and 1% BSA, followed by two washes with Dulbecco's phosphate-buffered saline (PBS) without calcium and magnesium (DPBS). Hepatocytes were purified by layering the cells over a 60% Percoll solution and centrifuged at 400*g* for 7 min at 4°C. The viability of hepatocytes was determined by Trypan blue exclusion. Purified hepatocytes were plated on collagen-coated plastic dishes in Williams' medium E supplemented with 1 μM insulin, 15 mM HEPES, 2 mM L-glutamine, penicillin (50 U/ml), streptomycin (50 μg/ml), and 10% fetal calf serum (FCS).

Hepatic resident macrophages (Kupffer cells) were isolated from livers of male adult Wistar rats by *in situ* collagenase perfusion as previously described (16, 17). In brief, following collagenase perfusion the nonparenchymal cell-enriched supernatant was centrifuged at 800*g* for 10 min at 4ºC and the obtained pellet was resuspended in DPBS and centrifuged again at 800*g* for 24 min through a 25/50% Percoll gradient at 4ºC. The interface of the gradient containing Kupffer and sinusoidal endothelial cells was seeded on either 35-mm tissue culture plates or 48-well plates and incubated at 37°C for 30 min. Cell monolayers adhered to the dishes were characterized as Kupffer cells by nonspecific esterase activity and by immunocytochemistry with the monoclonal antibody ED-2. Kupffer cells were cultured in RPMI 1640 medium supplemented with 2 mM L-glutamine, penicillin (50 U/ml), streptomycin (50 μg/ml), and 5% FCS.

CRL-2192 cells, a rat macrophage cell line (European Collection of Cell Cultures, Salisbury, UK), were grown in 24-well plates in RPMI 1640 medium supplemented with 2 mM L-glutamine, penicillin (50 U/ml), streptomycin (50 μg/ml), and 10% FCS and maintained in a humidified 5% CO_2 incubator at 37ºC. THP-1 cells, a monocytic human cell line, were grown in 75-cm^2 culture flasks in RPMI 1640 medium supplemented with 2 mM L-glutamine, penicillin (50 U/ml), streptomycin (50 μg/ml), and 10% FCS and maintained in a CO_2 incubator at 37ºC.

Cell incubations

Kupffer cells growing in 48-well plates were exposed to either vehicle (0.1% ethanol) or ASA (1 and 5 mM) for 20 min at 37ºC and stimulated with calcium ionophore A23187 (2 μM) for 20 min at 37ºC. In some experiments, Kupffer cells were exposed for 20 min to a selective COX-1 inhibitor (SC-560, 3 μM) or to a selective COX-2 inhibitor (celecoxib, 3 μM) and then stimulated with A23187 (2 μM) for 20 min at 37ºC. Supernatants from Kupffer cell incubations were immediately frozen and stored at –20ºC until further analysis of PGE_2, LTB_4, and 15-epi-LXA_4 levels by specific enzymeimmunoassays (EIAs). CRL-2192 cells (1×10^6 cells/ml) growing in 24-well plates were exposed to vehicle (0.1% ethanol) or increasing concentrations of ASA (0.1–5 mM), LXA_4 (100 nM), PGE_2 (300 nM), and LXA_4 (100 nM) in association with PGE_2 (300 nM) for 20 min at 37°C and then incubated with ionophore A23187 (2 μM) for additional 20 min at 37°C. In some experiments, CRL-2192 cells were exposed to macrophage-stimulating protein (MSP, 1 nM) for 24 h before the addition of the compounds. For measurements of 5-LO activity, incubations were terminated by the addition of cold methanol (2 vol) and the products were stored at –20 ºC until further analysis. Rat hepatocytes growing on collagen-coated P-100 plastic dishes ($3–12\times10^6$ cells/ml) were exposed to vehicle (0.1% ethanol), ASA (1 mM), LTB_4 (1 μM), 15-epi-LXA_4-methyl ester (1 μM), Wy-14643 (0.1 μM), PGE_2 (0.3 μM), PGE_2 (0.3 μM) in association with LTB_4 (1 μM), SC-560 (3 μM), or celecoxib (3 μM) for 24 h at 37°C.

Concentrations of the different eicosanoids and specifically for LXA_4 and 15-epi-LXA_4 were selected from references 18 and 19. THP-1 cells (2×10^6 cells/ml) were exposed to vehicle (0.1% ethanol) or ASA (1 mM) for 24 h at 37°C.

Analysis of 5-LO-derived eicosanoids by reverse-phase high-performance liquid chromatography (RP-HPLC)

Cellular samples were extracted by a solid-phase method. In brief, following the addition of PGB_2 (500 ng) as an internal standard, samples were centrifuged twice at 2000 rpm at 4ºC for 15 min and the supernatant was taken to dryness by rotoevaporation. Materials were resuspended in methanol-H_2O (1:45 vol/vol) by vortexing in a round-bottomed flask and transferred into a syringe, acidified to pH ~3.5 and loaded onto C_{18} silica reverse-phase cartridges. Materials were eluted from the cartridge with methyl formate, which was concentrated under a stream of N_2 and injected into a RP-HPLC system. This system consisted of a Waters (Milford, MA) integrated system controller (model 600E) equipped with a 996 Photodiode Array Detector and Millennium HPLC analysis software. The column, a Tracer Supelcosil (5 µm, 4.5×250 mm), was eluted with methanol/H_2O/acetic acid (65:35:0.01; v/v/v, pH 3.5) as phase one (t_0 –20 min) and a linear gradient with methanol/acetic acid (99.9:0.1, v/v) as phase two (20–45 min) at a flow rate of 1.0 ml/min. 5-LO activity was expressed as nanograms of 5-LO-derived products/10^6 cells that included LTB_4, the all-trans isomers of LTB_4 (6-*trans*-LTB_4 and 12-epi-6-*trans*-LTB_4), as well as 5*S*-HETE.

Measurement of PGE_2, LTB_4, 15-epi-LXA_4, and CINC-1 levels by EIA

PGE_2 and LTB_4 levels were measured in unextracted samples by highly specific EIAs from Cayman Chemical (Ann Harbor, MI). 15-epi-LXA_4 levels were determined by a highly specific EIA from Neogen (Lexington, KY). Concentrations of CINC-1 in supernatants from hepatocyte cultures were measured by a commercial EIA kit from Assay Designs (Ann Arbor, MI).

RNA isolation and reverse transcription-polymerase chain reaction (RT-PCR)

Total RNA was extracted by the guanidinium isothiocyanate-cesium chloride method (20). Samples were homogenized in guanidinium isothiocyanate (4 M), placed on cesium chloride (5.7 M), and centrifuged at 40,000 rpm for 20 h at 20°C. Subsequently, pellets from cell lysates were resuspended in TES solution (10 mmol/L Tris-HCl pH 7.4, 5 mmol/L EDTA, and 1% sodium dodecyl sulfate [SDS]), and the RNA was precipitated by the ethanol method and quantified by UV spectrophotometry. The integrity of RNA samples was documented by visualization of 18*S* and 28*S* ribosomal bands after electrophoresis through a denaturing 0.8% agarose gel stained with ethidium bromide. RT was performed with random primers by using AMV reverse transcriptase. PCR was performed using oligonucleotides designed from published rat COX-1, COX-2, 5-LO, 5-LO-activating protein (FLAP), and glyceraldehyde-3-phosphate dehydrogenase (GAPDH) cDNA sequences (21–24): COX-1, sense 5'-GTCATTCCCTGTTGTTACTATCC-3' and antisense 5'-CTCCCTTCTCAGCAGCAATCG-3'; COX-2, sense 5'-ACTTGCTCACTTTGTTGAGT CATTC-3' and antisense 5'-TTTGATTAGTACTGTAGGGTTAATG-3'; 5-LO, sense 5'-TACATTTACCTCAGCCTCATTG-3' and antisense 5'-GTCCACTCCCTTTTCACTATCA-3'; FLAP, sense 5'-GGGCTGATGTATCTGTTCGTG-3' and antisense 5'-

GCGGGGAGATCGTCGTGGTTA-3'; GAPDH, sense 5'-TCCCTCAAGATTGTCAGCAA-3' and antisense 5'-AGATCCACAACGGATACATT-3'. Oligonucleotides were synthesized by solid-phase phosphoramidite chemistry in a 394 DNA/RNA synthesizer (Applied Biosystems, Foster City, CA) in the DNA core facility of the Hospital Clínic. COX-1, COX-2, and GAPDH were amplified at 96ºC (30 s), 60ºC (1 min), and 72ºC (1 min) for 35 cycles. 5-LO and FLAP were amplified for 35 cycles at 94ºC (30 s), 58ºC (1 min), and 72ºC (30 s) and at 96ºC (30 s), 55ºC (30 s), and 72ºC (45 s), respectively. PCR products were analyzed by electrophoresis in 2% agarose gels and were visualized with ethidium bromide staining.

Protein isolation and Western blot analysis

Nuclear extracts were prepared according to the method of Schreiber et al. (25) with modifications. In brief, hepatocytes were washed in 5 ml of cold DPBS and centrifuged at 1100*g* for 5 min. The pellet was resuspended in 1 ml of DPBS, transferred into an Eppendorf tube, and pelleted again by spinning at 8000*g* for 15 s. The supernatant was removed, and the cell pellet was resuspended in 800 μl of cold buffer A (10 mM HEPES [pH 7.9], 10 mM KCl, 0.1 mM EDTA, 0.1 mM EGTA, 1 mM DTT, 0.5 mM PMSF, 1 μg/ml pepstatin, 1 μg/ml leupeptin, and 1 μg/ml aprotinin). Cells were allowed to swell on ice for 15 min, and then 50 μl of 0.5% IGEPAL was added and the tube was thoroughly mixed for 10 s. The homogenate was centrifuged at 8000*g* for 30 s, and the supernatant containing cytoplasm and RNA was saved at –80ºC. The nuclear pellet was resuspended in 100 μl of ice-cold buffer C (20 mM HEPES [pH 7.9], 400 mM NaCl, 1 mM DTT, 1 mM EDTA, 1 mM EGTA, 1 mM PMSF, 1 μg/ml pepstatin, 1 μg/ml leupeptin, and 1 μg/ml aprotinin). The tube was mixed thoroughly and placed on a rotatory shaker for 15 min and centrifuged at 11,000*g* for 5 min, and the supernatant containing the proteins from nuclear extracts was carefully transferred to a fresh tube. Western blot analyses for PPARα were performed by adding SDS-containing Laemmli sample buffer to 50 μg of protein as measured by the Bradford protein assay. Samples were subsequently heated for 5 min at 95ºC, electrophoresed through 12% SDS-polyacrylamide gels for 2 h at 150 V, and electroblotted onto membranes of polyvinylidene difluoride (PVDF). Gels were stained with Blue Coomassie to visualize loading differences, and membranes were submitted to Ponceau S staining to visualize the efficiency of the transfer. Membranes were then soaked for 1 h at 25ºC in Tris-buffered saline (TBS: 20 mM Tris-HCl [pH 7.4] and 0.5 M NaCl) containing 5% (w/v) nonfat dry milk. Blots were incubated for 1 h at 25ºC with the primary anti-murine PPARα antiserum (1:500 dilution) in 0.25% (v/v) Tween 20 in TBS (0.25% T-TBS) containing 0.1% dry milk. After successive washes (5 min in TBS, three times for 6 min in 0.25% T-TBS and then 5 min in TBS), blots were incubated for 1 h at 25ºC with a horseradish peroxidase-linked donkey anti-rabbit antibody (1:2000 dilution) in 0.25% T-TBS containing 0.1% dry milk. The blots were finally washed as previously described and subsequently developed using the enhanced chemiluminescence (ECL) Western blot analysis system.

Synthetic LTB_4, PGE_2, 5*S*-HETE, PGB_2, 20-OH-LTB_4, and Wy-14643 were from Cayman Chemical (Ann Harbor, MI). LXA_4 was from Cascade Biochem (Reading, UK). 15-epi-LXA_4-methyl ester was a gift from Professor Charles N. Serhan (Center for Experimental Therapeutics and Reperfusion Injury, Brigham and Women's Hospital, Harvard Medical School, Boston, MA). SC-560 and celecoxib were kindly provided by Pharmacia Research and Development (St. Louis, MO).

Aspirin, ionophore A23187, guanidinium isothiocyanate, Williams' medium E and Tracer Supelcosil HPLC columns were purchased from Sigma (St. Louis, MO). Cesium chloride and collagenase (A type) were from Roche (Mannheim, Germany). Percoll was from Pharmacia (Uppsala, Sweden). HPLC grade solvents were from Ferosa (Barcelona, Spain), and methyl formate was from Merck (Darmstadt, Germany). Sep-Pak C_{18} cartridges were purchased from Waters. Taq DNA polymerase, FCS, DPBS, and HBSS were from Invitrogen (Carlsbad, CA). The first strand cDNA synthesis kit was from Promega (Madison, WI), and the ECL system was from Amersham (Buckinghamshire, UK). MSP was from R&D Systems (Minneapolis, MN). The rabbit anti-murine PPARα antiserum was from Alexis (San Diego, CA), and the ED-2 monoclonal antibody was from Serotec (Raleigh, NC).

RESULTS AND DISCUSSION

Rat Kupffer cells isolated by *in situ* collagenase perfusion assumed an even distribution over the culture substratum within 24 h. Under basal culture conditions, rat Kupffer cells constitutively expressed COX-1, COX-2, 5-LO, and FLAP mRNA (Fig. 1A). Once we determined which eicosanoid-generating enzymes were present in Kupffer cells, we tested the impact of ASA on the biosynthesis of arachidonic acid-derived products in these liver resident macrophages. As shown in Figure 1B (left panel), addition of increasing concentrations of ASA to Kupffer cells significantly inhibited prostanoid (e.g., PGE_2) release. The inhibitory effect of ASA on COX-derived products was associated with a dose-dependent increase of the 5-LO product LTB_4 (Fig. 1B, middle panel). These findings are in agreement with human studies reporting an increase in the circulating levels of LTs following COX inhibition, probably secondary to the shunting of arachidonic acid to the 5-LO-initiated pathway (26, 27). Alternatively and according to a recent investigation by Levy et al. (28), the increase in LTB_4 formation following ASA treatment may be secondary to abolishment of the inhibitory action exerted by COX-derived products (including PGE_2) on LTB_4 biosynthesis. Because both COX-2 and 5-LO are present in Kupffer cells, we also examined the formation of a member of the novel class of ASA-triggered 15*R* containing LXs (15-epi-LXA_4) in rat Kupffer cells. As expected, detectable amounts of 15-epi-LXA_4 (102.8 ± 13.5 pg/ml) were found in Kupffer cell supernatants in comparable levels as PGE_2 (161 ± 32 pg/ml) and LTB_4 (2.6 ± 0.5 pg/ml). Interestingly, in these liver macrophages, there was an inverse relationship between the dose-dependent ASA-triggered 15-epi-LXA_4 biosynthesis (Fig. 1B, right panel) and PGE_2 formation (Fig. 1B, left panel). This phenomenon was specific to ASA action because neither the selective COX-1 inhibitor SC-560 (from 41.1 ± 5.3 to 57.7 ± 5.6 pg/incubation) nor the selective COX-2 inhibitor celecoxib (from 41.1 ± 5.3 to 52.9 ± 10.4 pg/incubation) stimulated 15-epi-LXA_4 biosynthesis in rat Kupffer cells. Note that PGE_2 formation was significantly inhibited by SC-560 (from 64.4 ± 12.7 to 35.9 ± 9.3 pg/incubation, $P<0.05$) but not by celecoxib (64.4 ± 12.7 to 56.3 ± 19.9 pg/incubation), suggesting that most of PGE_2 released by Kupffer cells is likely to be generated via the COX-1-initiated pathway. Taken together, these findings are consistent with the notion that although the primary effect of ASA is the inhibition of COX with a consequent reduction of PG formation, this NSAID also has significant effects on other pathways for arachidonic acid metabolism (i.e., LTB_4 and 15-epi-LXA_4 biosynthesis).

The impact of ASA treatment on macrophage arachidonic acid metabolism was further characterized in CRL-2192 cells. In this rat macrophage cell line, we first analyzed COX-1, COX-2, 5-LO, and

FLAP mRNA expression by RT-PCR. As shown in Figure 2A, under resting conditions, CRL-2192 cells displayed constitutive mRNA expression for COX-1, 5-LO, and FLAP. COX-2 was not expressed constitutively in CRL-2192 cells, although a faint band for COX-2 was detected after stimulation with proinflammatory factors such as LPS (10 ng/ml, 18 h) (data not shown) or cytokine/growth factors such as MSP, a hepatocyte-derived serum protein involved in macrophage activation (29) (Fig. 2A). The presence of COX-2 mRNA expression was observed as early as 6 h following MSP treatment (data not shown). Similar to what occurs in Kupffer cells, the addition of ASA to cultures of resting rat CRL-2192 cells significantly increased LTB_4 formation (Fig. 2B). This ASA-induced increase in LTB_4 levels was dose-dependent and was maximal at millimolar concentrations (Fig. 2B). As shown in Figure 2C, the release of 5-LO products by CRL-2192 cells was further increased when ASA was added to cultures previously exposed to MSP. MSP alone had no effect on 5-LO activity in CRL-2192 cells (Fig. 2C). Interestingly, LXA_4, an endogenous eicosanoid that carries "stop signals" for inflammation and is generated via biosynthetic pathways that involve the dual lipoxygenation of arachidonic acid by either 5- and 15-LO or 5- and 12-LO (12), significantly inhibited 5-LO activity in CRL-2192 cells (Fig. 2D). Both PGE_2 alone and PGE_2 in association with LXA_4 also significantly decreased 5-LO activity in this rat macrophage cell line. Levy et al. recently reported in human neutrophils that PGE_2 induces a switch in eicosanoid biosynthesis from the predominantly LTB_4 and 5-LO-initiated pathway to LXA_4 (28). Our findings demonstrating that in rat macrophages LXA_4 inhibits 5-LO activity to a similar extent as PGE_2 suggest that this endogenous antiinflammatory eicosanoid also plays an active role in the switching of eicosanoid classes possibly during resolution of inflammation.

To ascertain the biological significance of ASA actions in rat macrophages, we put our findings into the context of the liver sinusoid where Kupffer cells are in close contact with hepatocytes. In particular, we were interested in examining the influence of ASA and Kupffer cell-derived arachidonic acid products on gene transcriptional factors implicated in the control of inflammation. One group of such transcriptional regulators is the PPAR family, which is comprised of three subtypes: PPARα, PPARδ, and PPARγ (30). Given that the predominant PPAR in hepatocytes is PPARα (31), we focused our investigation on this PPAR subtype. As shown in Figure 3A and as compared to vehicle, ASA significantly reduced PPARα protein levels in rat hepatocytes. The 5-LO-derived product, LTB_4, as well as 15-epi-LXA_4 and the selective PPARα agonist activator Wy-14643, also decreased PPARα levels in rat hepatocytes (Fig. 3A). The observation that ASA decreases PPARα protein expression in rat hepatocytes was further confirmed in nuclear extracts from THP-1 cells (Fig. 3B), indicating that this ASA property is not restricted to the liver scenario. Conversely and as shown in Figure 3C, PGE_2 alone and PGE_2 in association with LTB_4 did not induce any change in PPARα protein expression in rat hepatocytes. Similarly, PPARα levels in rat hepatocyte cultures were not modified by the addition of the selective COX inhibitors celecoxib and SC-560 (Fig. 3C).

The reduction of PPARα levels by ASA may have important consequences in the inflammatory response. In this regard, the PPAR family of transcriptional regulators has been shown to modulate various genes involved in inflammation, including members of the IL-8 family such as CINC-1 (32, 33). On the basis of these data, we examined the effect of ASA and Kupffer cell-derived arachidonic acid products on CINC-1 release by rat hepatocytes in culture. CINC-1 is a 8-kDa proinflammatory peptide and a member of the C-X-C family of chemokines, with potent

chemotactic activity toward neutrophils (34, 35). CINC-1 is the rat counterpart of human IL-8 and/or growth-regulated gene product α (GROα) (34, 35). As shown in Figure 4, and unlike LTB_4 and PGE_2 alone, the addition of LTB_4 in association with PGE_2 significantly increased CINC-1 secretion by rat hepatocytes. In sharp contrast, CINC-1 concentrations were significantly reduced by ASA (Fig. 4). The mechanism by which ASA down-regulates CINC-1 secretion is presently unknown, although the selective PPARα agonist activator Wy-14643 also reduced hepatocyte CINC-1 production (Fig. 4), implying the action of ASA at the level of PPARα. Moreover, the endogenous antiinflammatory compound 15-epi-LXA_4, whose biosynthesis is triggered by ASA, also consistently inhibited CINC-1 release by rat hepatocytes (Fig. 4). These results are similar to those of Gronert et al., who previously established that LXA_4 and LXA_4 stable analogs are potent inhibitors of enterocyte cytokine-induced IL-8 release (36). Finally, note that celecoxib but not SC-560 decreased the release of CINC-1 by rat hepatocytes to a similar extent as ASA (Fig. 4). These data showing that a selective COX-2 inhibitor modulates CINC-1 production by rat hepatocytes are in disagreement with those previously reported by Pang et al. implicating both COX-1 and COX-2 in chemokine secretion in human airway smooth muscle cells (37).

The actions of ASA on liver cell arachidonic acid metabolism are summarized in Figure 5. In Kupffer cells, ASA inhibits COX and PGE_2 biosynthesis and favors the oxidation of arachidonic acid via the 5-LO pathway (e.g., LTB_4). In addition, ASA triggers the generation of the endogenous antiinflammatory eicosanoid 15-epi-LXA_4 in these liver resident macrophages. Biosynthesis of LXA_4 and 15-epi-LXA_4 in response to ASA may also occur by transcellular routes involving hepatocytes and nonparenchymal liver cells (e.g., Kupffer cells and endothelial cells) as previously demonstrated by Titos et al. (15). These endogenous antiinflammatory lipid mediators, in turn, have the ability to inhibit 5-LO activity in Kupffer cells (to a similar extent as PGE_2) and to reduce PPARα protein expression and CINC-1 secretion in underlying hepatocytes. Interestingly, ASA directly decreases PPARα levels and CINC-1 secretion in hepatocytes. In contrast, LTB_4 together with PGE_2 generated by Kupffer cells up-regulate CINC-1 production in adjacent hepatocytes. Taken together, these results provide new insight regarding the molecular mechanisms underlying the pleiotropic response to ASA.

ACKNOWLEDGMENTS

These studies were supported in part by Comisión Interministerial de Ciencia y Tecnología (SAF 00/0043) and Fondo de Investigaciones Sanitarias (FIS 00/0616 and 02/0029). A. Planagumà was supported by a fellowship from IDIBAPS. E. Titos and M. López-Parra received a fellowship from Ministerio de Sanidad y Consumo (BEFI 98/9314) and Ministerio de Ciencia y Tecnología, respectively. The authors are indebted to Professor Charles N. Serhan (Center for Experimental Therapeutics and Reperfusion Injury, Brigham and Women's Hospital, Harvard Medical School, Boston, MA) for providing the 15-epi-LXA_4-methyl ester and helpful discussions. The authors thank Montse Bernat for technical assistance.

REFERENCES

1. Payan, D. G., and Katzung, B.G. (1995) Nonsteroidal antiinflammatory drugs; nonopioid analgesics; drugs used in gout. In *Basic & Clinical Pharmacology* (Katzung, B. G., ed.), pp. 538–559, Appleton & Lange, Norwalk, CT

2. Patrono, C. (1996) Aspirin as an antiplatelet drug. *N. Engl. J. Med.* **330,** 1287–1294

3. Grilli, M., Pizzi, M., Memo, M., and Spano, P. (1996) Neuroprotection by aspirin and sodium salicylate through blockade of NF-κB. *Science* **274,** 1383–1385

4. Thun, M. J., Namboodiri, M. M., and Heath C. W. (1991) Aspirin use and reduced risk of fatal colon cancer. *N. Engl. J. Med.* **325,** 1593–1596

5. Vane, J. R. (1971) Inhibition of prostaglandin synthesis as a mechanism of action for the aspirin-like drugs. *Nature* **231,** 232–235

6. Jurivich, D. A., Sistonen, L., Kroes, R. A., and Morimoto, R. I. (1992) Effect of sodium salicylate on the human heat shock response. *Science* **255,** 1243–1245

7. Schwenger, P., Alpert, D., Skolnik, E. Y., and Vilcek, J. (1998) Activation of p38 mitogen-activated protein kinase by sodium salicylate leads to inhibition of tumor necrosis factor-induced IκBα phosphorylation and degradation. *Mol. Cell. Biol.* **18,** 78–84

8. Pillinger, M. H., Capodici, C., Rosenthal, P., Kheterpal, N., Hanft, S., Philips, M. R., and Weissmann, G. (1998) Modes of action of aspirin-like drugs: salicylates inhibit Erk activation and integrin-dependent neutrophil adhesion. *Proc. Natl. Acad. Sci.* USA **95,** 14540–14545

9. Koop, E., and Ghosh, S. (1994) Inhibition of NF-κB by sodium salicylate and aspirin. *Science* **265,** 956–959

10. Dong, Z., Huang, C., Brown, E., and Ma, W.-Y. (1997) Inhibition of activator protein 1 activity and neoplastic transformation by aspirin. *J. Biol. Chem.* **272,** 9962–9970

11. Clària, J., and Serhan, C. N. (1995) Aspirin triggers previously unrecognized bioactive eicosanoids by human endothelial cell-leukocyte interaction. *Proc. Natl. Acad. Sci. USA*. **92,** 9475–9479

12. Serhan, C. N. (1997) Lipoxins and novel aspirin-triggered 15-epi-lipoxins (ATL): a jungle of cell-cell interactions or a therapeutic opportunity? *Prostaglandins* **53,** 107–137

13. Bochner, F., Williams, D. B., Morris, P. M., Siebert, D. M., and Lloyd J. V. (1988) Pharmacokinetics of low-dose oral modified release, soluble and intravenous aspirin in man and effects on platelet functions. *Eur. J. Clin. Pharmacol.* **35,** 287–294

14. Kim, D., Yang, H. Y. S., and Jakoby, W. B. (1990) Aspirin hydrolyzing esterases from rat liver cytosol. *Biochem. Pharmacol.* **40,** 481–487

15. Titos, E., Chiang, N., Serhan, C. N., Romano, M., Gaya, J., Pueyo, G., and Clària, J. (1999) Hepatocytes are a rich source of novel aspirin-triggered 15-epi-lipoxin A_4. *Am. J. Physiol.* **277,** C870–C877

16. Berry, M. N., and Friend, D. S. (1969) High yield preparation of isolated rat liver parenchymal cells. A biochemical and fine study. *J. Cell. Biol.* **43,** 506–520

17. Titos, E., Clària, J., Bataller, R., Bosch-Marcé, M., Ginès, P., Jiménez, W., Arroyo, V., Rivera, F., and Rodés, J. (2000) Hepatocyte-derived cysteinyl leukotrienes modulate vascular tone in experimental cirrhosis. *Gastroenterology* **119,** 794–805

18. Serhan, C. N., Maddox, J. F., Petasis, N. A., Akritopoulou-Zanze, I., Papayianni, A., Brady, H. R., Colgan, S. P., and Madara, J. L. (1995) Design of lipoxin A_4 stable analogs that block transmigration and adhesion of human neutrophils. *Biochemistry* **34,** 14609–14615

19. Devchand, P. R., Keller, H., Peters, J. M., Vazquez, M., Gonzalez, F.J., and Wahli, W. (1996) The PPARα-leukotriene B_4 pathway to inflammation control. *Nature* **384,** 39–43

20. Chirgwin, J. M., Pryzbyla, R. J., McDonald, R. J., and Rutter, W. J. (1978) Isolation of biologically active ribonucleic acid from sources enriched in ribonuclease. *Biochemistry* **18,** 5294–5299

21. Feng, L., Sun, W., Xia Y., Tang, W.W., Chanmugam, P., Soyoola, E, Wilson, C. B., and Hwang, D. (1993) Cloning two isoforms of rat cyclooxygenase: differential regulation of their expression. *Arch. Biochem. Biophys.* **307,** 361–368

22. Balcarek, J.M., Theisen, T. W., Cook, M. N., Varrichio, A., Hwang S-M, Strohsacker, M. W., and Crooke, S. T. (1988) Isolation and characterization of a cDNA clone encoding rat 5-lipoxygenase. *J. Biol. Chem.* **263,** 13937–13941

23. Dixon, R. A. F., Diehl, R. E., Opas, E., Rands, E., Vickers, P. J., Evans, J. F., Gillard, J.W., and Miller, D. K. (1990) Requirement of a 5-lipoxygenase-activating protein for leukotriene synthesis. *Nature* **343,** 282–284

24. Fort, P., Marty, L., Piechacyk, M., Sabrouty, S. E., Dani, C., Janteur, P., and Blanchard, J. M. (1985) Various rat adult tissues express only one major mRNA species from glyceraldehyde-3-phosphate-dehydrogenase multigene family. *Nucleic Acids Res.* **13,** 1431–1442

25. Schreiber, E., Matthias, P., Muller, M. M., and Schaffner, W. (1989) Rapid detection of octamer binding proteins with "mini-extracts" prepared from a small number of cells. *Nucleic Acids Res.* **17,** 6419–6420

26. Brezinsky, D. A., Nesto, R. W., and Serhan, C. N. (1992) Angioplasty triggers intracoronary leukotrienes and lipoxin A_4. Impact of aspirin therapy. *Circulation* **86,** 56–63

27. Engström, K., Wallin, R., and Saldeen, T. (2001) Effect of low-dose aspirin in combination with stable fish oil on whole blood production of eicosanoids. *Prostaglandins Leukot. Essent. Fatty Acids* **64,** 291–297

28. Levy, B. D., Clish, C. B., Schmidt, B., Gronert, K., and Serhan, C. N. (2001) Lipid mediator class switching during acute inflammation: signals in resolution. *Nature Immunol.* **2,** 612–619

29. Skeel, A. H., Yohimura, T., Showelter, D., Tanaka, S., Appell, E., and Leonard, E. J. (1991) Macrophage stimulating protein: purification, partial amino acid sequences and cellular activity. *J. Exp. Med.* **173,** 1227–1234

30. Chinetti, G., Fruchart, J-C., and Staels, B. (2000) Peroxisome proliferator-activated receptors (PPARs): nuclear receptors at the crossroads between lipid metabolism and inflammation. *Inflamm. Res.* **49,** 497–505

31. Braissant, O., Foufelle, F., Scotto, C., Dauca, M., and Wahli, W. (1996) Differential expression of peroxisome proliferator-activated receptors (PPARs): tissue distribution of PPAR-alpha, -beta, and -gamma in the adult rat. *Endocrinology* **137,** 354–366

32. Wang, A. C. C., Dai, X., Luu, B., and Conrad, D. J. (2001). Peroxisome proliferator-activated receptor γ regulates airway epithelial cell activation. *Am. J. Respir. Cell. Mol. Biol.* **24,** 688–693

33. Lee, H., Shi, W., Tontonoz, P., Wang, S., Subbanagounder, G., Hedrick, C. C., Hama S., Borromeo, C., Evans, R. M., Berliner, J. A., and Nagy, L. (2000) Role for peroxisome proliferator-activated receptor alpha in oxidized phospholipid-induced synthesis of monocyte chemotactic protein-1 and interleukin-8 by endothelial cells. *Circ. Res.* **87,** 516–521

34. Watanabe, K., Koizumi, F., Kurashige, Y., Tsurufuji, S., and Nakagawa, H. (1991) Rat CINC, a member of the interleukin-8 family, is a neutrophil-specific chemoattractant *in vivo*. *Exp. Mol. Pathol.* **55,** 30–37

35. Watanabe, K., Konishi, K., Fujioka, M., Kinoshita, S., and Nakagawa, H. (1989) The neutrophil chemoattractant produced by the rat kidney epitheliod cell line NRK-53E is a protein related to the KC/gro protein. *J. Biol. Chem.* **264,** 19559–19563

36. Gronert, K., Gewirtz, A., Madara, J. L., and Serhan, C. N. (1998) Identification of a human enterocyte lipoxin A_4 receptor that is regulated by interleukin (IL)-13 and interferon γ and inhibits tumor necrosis factor α-induced IL-8 release. *J. Exp. Med.* **187,** 1285–1294

37. Pang, L., and Knox, A. J. (1998) Bradykinin stimulates IL-8 production in cultured human airway smooth muscle cells: role of cyclooxygenase products. *J. Immunol.* **161**, 2509–2515

Received March 13, 2002; accepted August 20, 2002.

Fig. 1

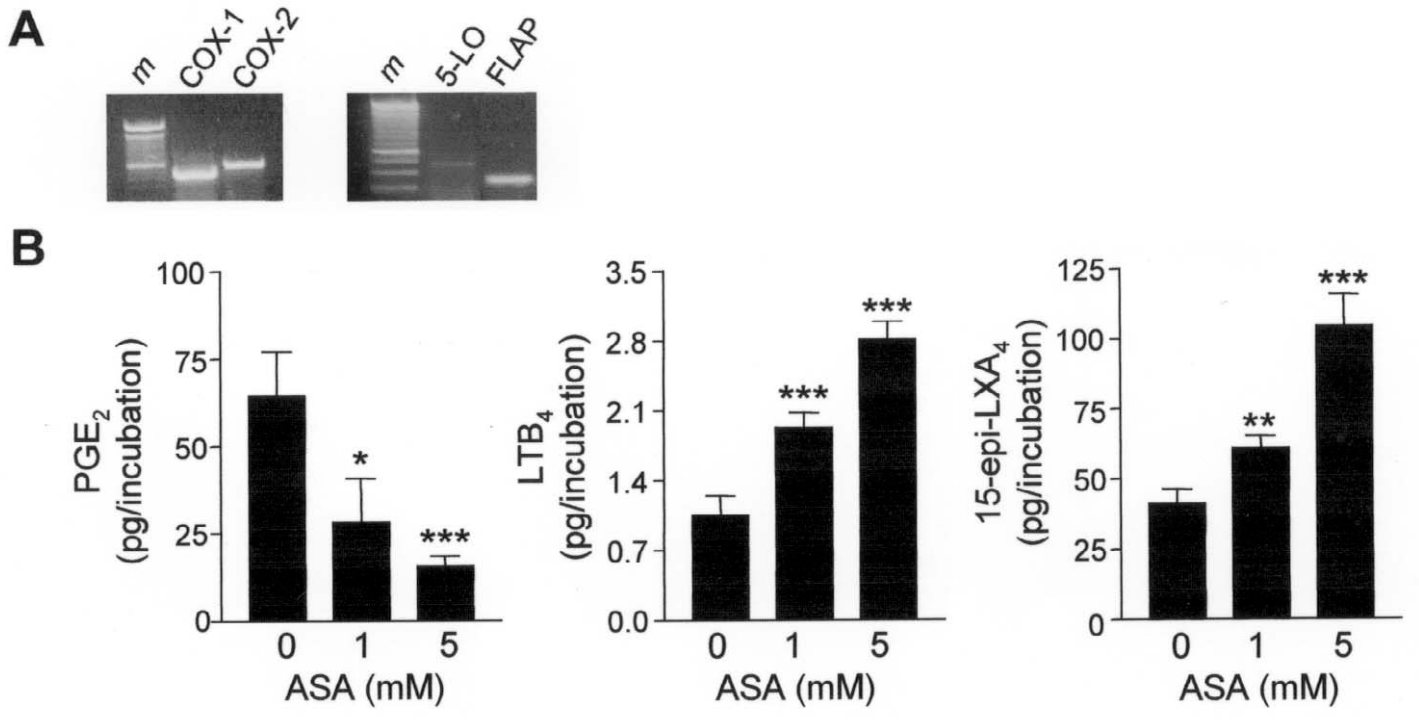

Figure 1. A) Detection of COX-1, COX-2, 5-LO, and FLAP mRNA expression by reverse transcription-polymerase chain reaction (RT-PCR) in rat Kupffer cells. RNA was obtained by the guanidinium isothiocyanate-cesium chloride method, and cDNA was produced by RT. PCR amplification was performed using specific oligonucleotide sequences of rat COX-1, COX-2, 5-LO, and FLAP, and PCR products were visualized by ethidium bromide staining. *m*, molecular weight DNA ladder. **B)** Effect of aspirin (ASA) on PGE_2 (upper panel), LTB_4 (middle panel), and 15-epi-LXA_4 (lower panel) biosynthesis in rat Kupffer cells. Kupffer cells growing in 48-well tissue culture plates were treated with increasing doses of ASA (0, 1, and 5 mM) for 20 min at 37°C and were then exposed to A23187 (2 μM) for an additional 20 min. PGE_2, LTB_4, and 15-epi-LXA_4 levels were measured by specific enzymeimmunoassays (EIA). Results represent the mean ±SE of 11 different experiments. **P*<0.05, ***P*<0.025, and ****P*<0.005 vs. vehicle.

Fig. 2

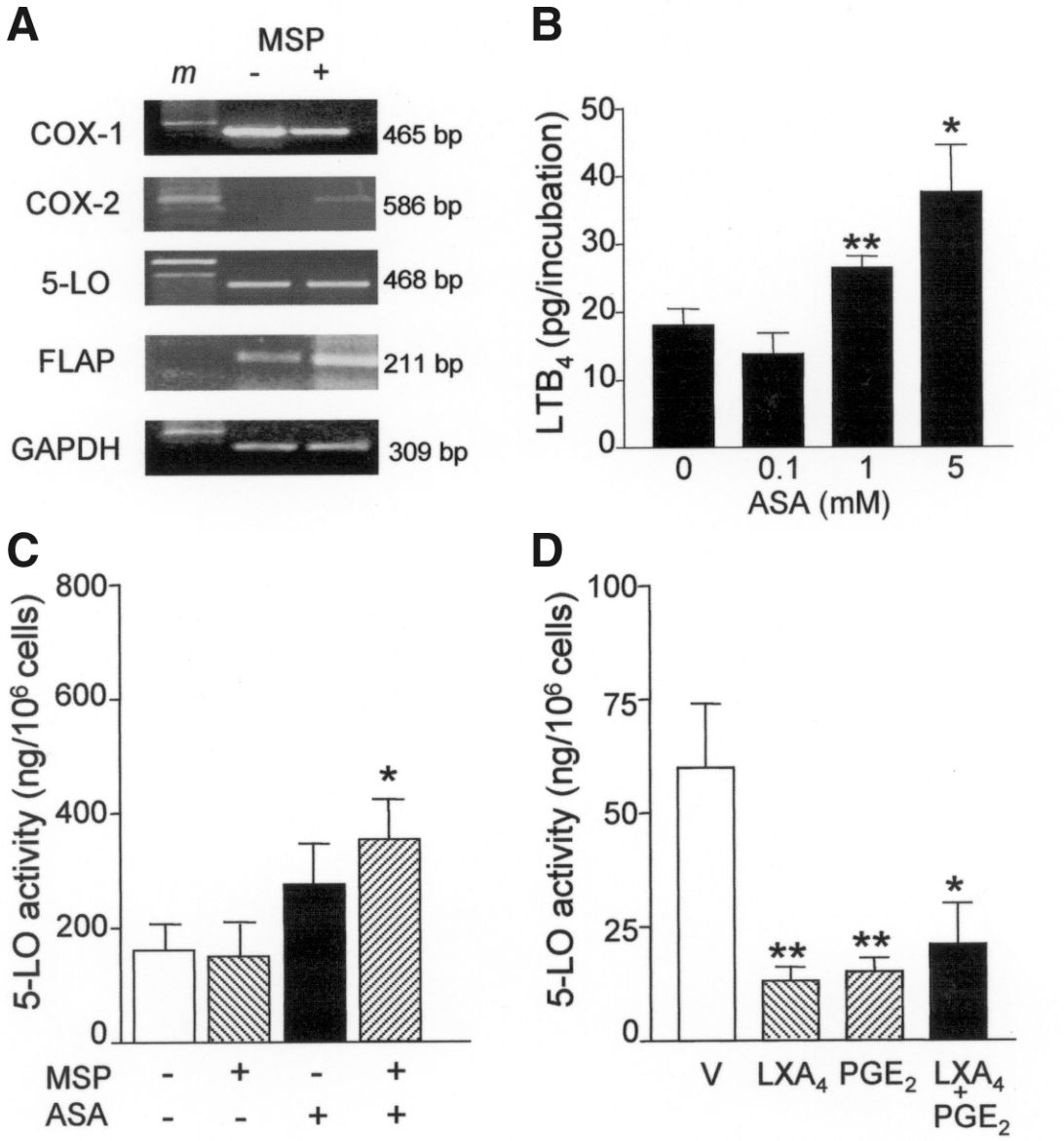

Figure 2. A) Detection of COX-1, COX-2, 5-LO, and FLAP mRNA expression by RT-PCR in rat CRL-2192 cells incubated with or without macrophage stimulating protein (MSP) for 24 h. RT-PCR amplification was performed as described in **Figure 1** and in Materials and Methods. *m*, molecular weight DNA ladder. **B)** Effect of ASA on LTB_4 formation by rat CRL-2192 cells. CRL-2192 cells (1×10^6 cells/ml) were exposed to increasing concentrations of ASA (0, 0.1, 1, and 5 mM) for 20 min at 37°C and were then incubated with ionophore A23187 (2 μM) for an additional 20 min. LTB_4 levels were measured by EIA. Results represent the mean ±SE of 4 different experiments with duplicate determinations. **P*<0.05 and ***P*<0.025 vs. vehicle. **C)** Effect of ASA on 5-LO activity in rat CRL-2192 cells in the absence or presence of MSP. CRL-2192 cells were exposed to vehicle (0.1% ethanol) or MSP (1 nM) for 24 h, treated with vehicle (0.1% ethanol) or ASA (1 mM) for 20 min at 37°C, and then incubated with ionophore A23187 (2 μM) for an additional 20 min. Incubations were terminated by the addition of cold methanol, and 5-LO products were analyzed by reverse-phase high-performance liquid chromatography (RP-HPLC). Results represent the mean ±SE of seven different experiments. **P*<0.05 vs. vehicle. **D)** Effect of LXA_4 and PGE_2 on 5-LO activity in rat CRL-2192 cells. CRL-2192 cells were exposed to either vehicle (0.1% ethanol), LXA_4 (100 nM), PGE_2 (300 nM), or LXA_4 (100 nM) in association with PGE_2 (300 nM) for 20 min at 37°C and were then incubated with ionophore A23187 (2 μM) for an additional 20 min. 5-LO products were determined by RP-HPLC. Results represent the mean ±SE of six different experiments. **P*<0.05 and ***P*<0.025 vs. vehicle.

Fig. 3

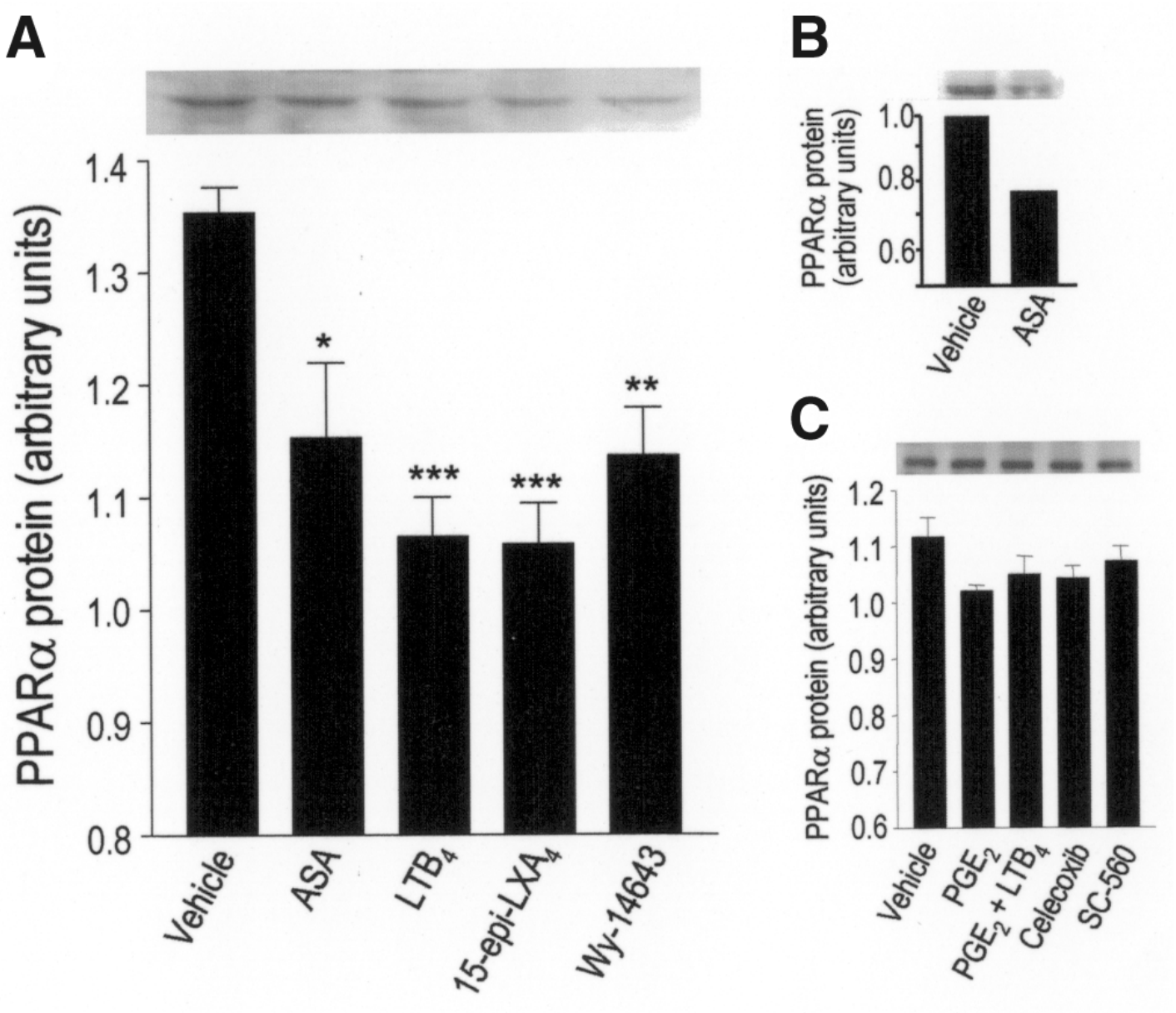

Figure 3. Effect of ASA and Kupffer cell-derived arachidonic acid metabolites on peroxisome proliferator-activated receptor α (PPARα) protein expression in rat hepatocytes. A) Rat hepatocytes growing on collagen-coated P-100 plastic dishes ($3–12\times10^6$ cells/ml) were exposed to either vehicle (0.1% ethanol), 1 mM ASA, 1 μM LTB_4, 1 μM 15-epi-LXA_4-methyl ester, or 0.1 μM Wy-14643 for 24 h at 37°C. Nuclear extracts were electrophoresed and probed with a specific anti-murine PPARα antiserum, and band intensities were determined by scanning densitometry. **B)** Human mononuclear leukocytes (THP-1 cells) (2×10^6 cells/ml) were exposed to vehicle (0.1% ethanol) or 1 mM ASA for 24 h at 37°C, and nuclear extracts were analyzed by Western blot as described previously. **C)** Rat hepatocytes growing on collagen-coated plastic dishes were exposed to either vehicle (0.1% ethanol), 0.3 μM PGE_2, 0.3 μM PGE_2 in association with 1 μM LTB_4, 3 μM celecoxib, or 3 μM SC-560 for 24 h at 37°C. Nuclear extracts were electrophoresed and probed as described previously. Results are representative of 12 separate experiments. *P<0.05, **P<0.005, and ***P<0.001 vs. vehicle.

Fig. 4

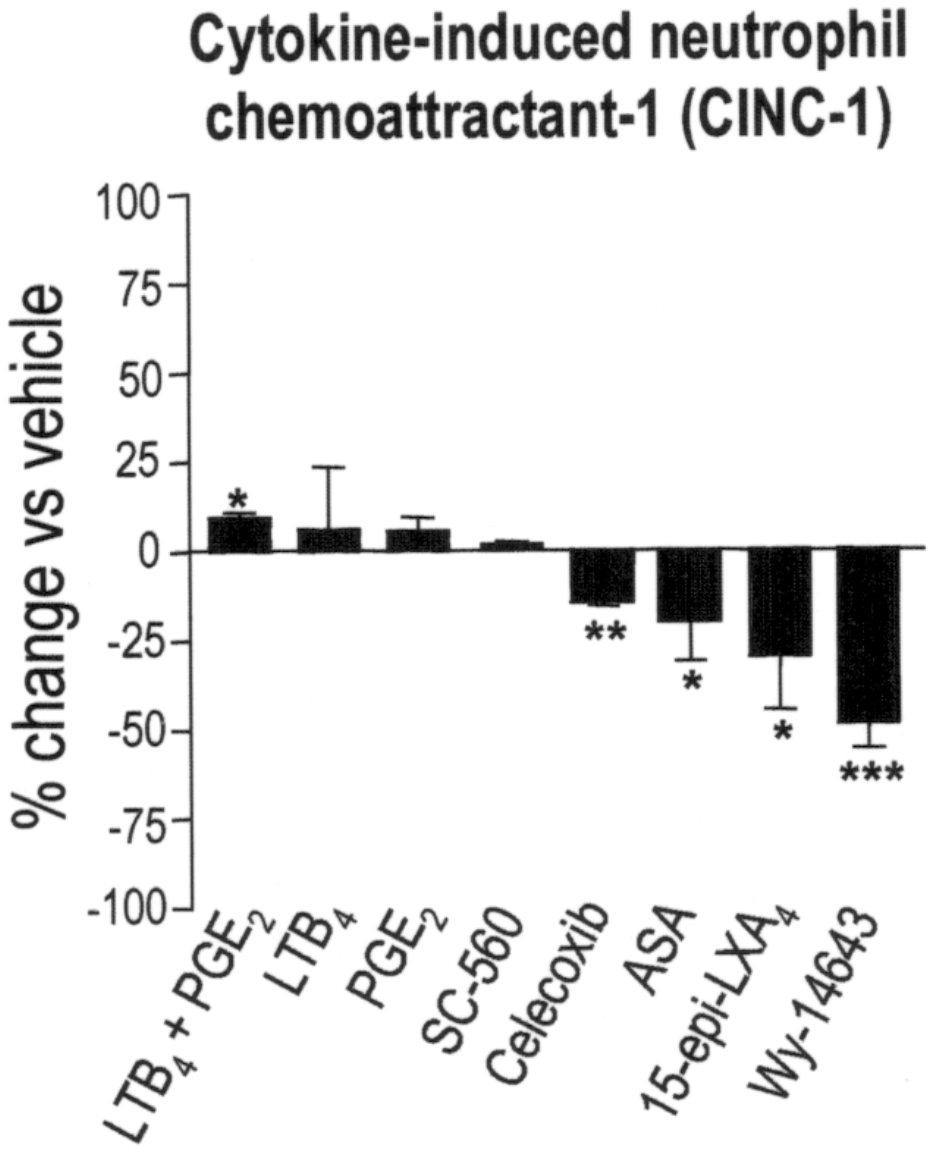

Figure 4. Effect of ASA and Kupffer cell-derived arachidonic acid metabolites on CINC-1 release in rat hepatocytes. CINC-1 concentrations were determined by EIA in supernatants from hepatocytes exposed to either vehicle (0.1% ethanol), 1 μM LTB_4, 0.3 μM PGE_2, 1 μM LTB_4 in association with 0.3 μM PGE_2, 3 μM SC-560, 3 μM celecoxib, 1 mM ASA, 1 μM 15-epi-LXA_4-methyl ester, or 0.1 μM Wy-14643 for 24 h at 37°C. Results show the mean ±SE of 11 different experiments with duplicate determinations. **P*<0.05; ***P*<0.005, and ****P*<0.001 vs. vehicle.

Fig. 5

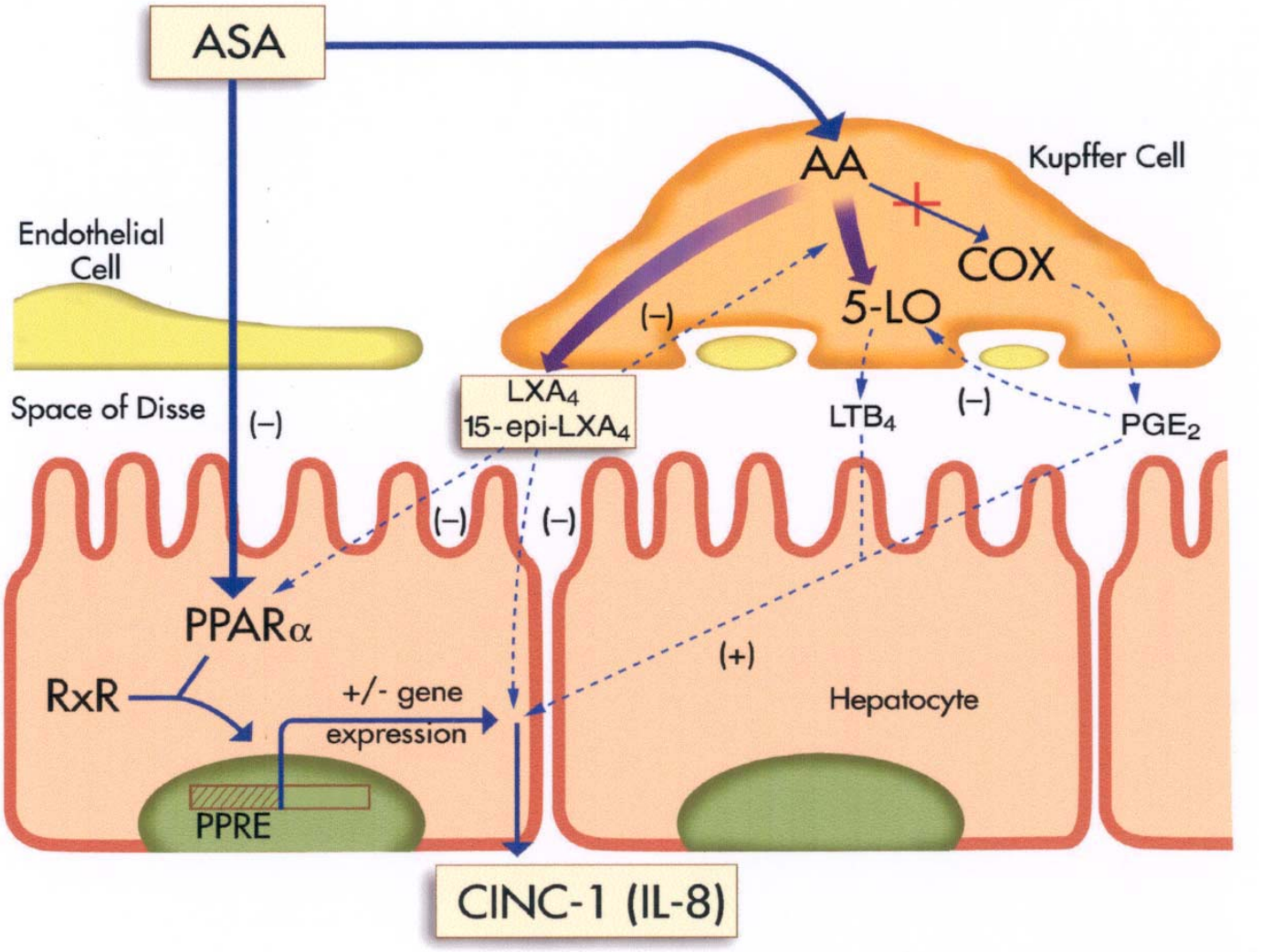

Figure 5. Hypothetical scheme of ASA actions in rat liver sinusoidal cells. In Kupffer cells, ASA inhibits COX and PG biosynthesis and favors the oxidation of arachidonic acid via the 5-LO pathway (e.g., LTB_4). In these liver resident macrophages, ASA also switches the metabolism of arachidonic acid to the biosynthesis of LXA_4 and ASA-triggered 15-epi-LXA_4. These endogenous anti-inflammatory mediators in turn inhibit 5-LO activity (to a similar extent as PGE_2) in Kupffer cells and reduce PPARα protein expression and CINC-1 secretion in underlying hepatocytes. However, ASA directly decreases PPARα levels in hepatocytes. PPARα heterodimerizes with the retinoid X receptor (RxR) and subsequently binds to specific DNA motifs (peroxisome proliferator-responsive elements [PPRE]) located within the promoter region of target genes, including the member of the interleukin-8 (IL-8) family CINC-1. Indeed, in rat hepatocytes treated with ASA, inhibition of PPARα levels is associated with a decrease in CINC-1 release. In contrast, LTB_4 in association with PGE_2 generated by Kupffer cells stimulates CINC-1 release in adjacent hepatocytes.

ARTICLE 2

L'inhibidor selectiu de la ciclooxigenasa-2 SC-236 redueix la fibrosi hepàtica per mecanismes que involucren apoptosi i activació del PPARγ en cèl·lules no parenquimals

1. L'expressió de la proteïna de COX-2 es troba incrementada en fetges de rates tractades amb tetraclorur de carboni (CCl_4).

Es va detectar per immunohistoquímica una inducció marcada de l'expressió de la proteïna de COX-2 en fetges de rates tractades amb CCl_4 en comparació amb els fetges de rates controls.

2. L'inhibidor selectiu de la COX-2, l'SC-236, redueix la fibrosi hepàtica en rates tractades amb CCl_4.

Després de l'administració de CCl_4, les rates van desenvolupar esteatosi hepàtica, inflamació, increment del volum dels hepatòcits i necrosi. A la sisena setmana de tractament amb CCl_4, l'arquitectura del fetge es presenta extensament desorganitzada amb una pèrdua de l'estructura dels sinusoides. Es poden observar petites àrees d'hepatòcits sans envoltades per deposicions de col·lagen i ponts septals a les regions porta. L'administració de SC-236 a rates tractades amb CCl_4 va exercir un efecte antifibròtic significant, com es revela de l'anàlisi histològic de les seccions de fetge i de la presència d'un baix contingut hepàtic d'hidroxiprolina (13.0 ± 1.4 *versus* 16.9 ± 1.4 nmol/mg teixit hepàtic, $P<0.05$), un marcador establert de síntesi de col·lagen.

3. El SC-236 disminueix l'activitat de la metaloproteasa (MMP)-2 i MMP-9 i l'expressió de la proteïna de l'actina de múscul llis (SMA)-α.

A causa de que les MMPs són enzims clau en la regulació del remodelatge de la matriu extracel·lular i les seves activitats es correlacionen estretament amb la severitat de la fibrosi hepàtica, vam determinar les activitats hepàtiques de la MMP-2 i la MMP-9 per zimografia. El SC-236 va reduir significativament l'activitat gelatinolítica de la MMP-2 hepàtica i va abolir completament l'activitat de la MMP-9 en rates tractades amb CCl_4. A més a més, el SC-236 va suprimir consistentment l'expressió de la proteïna del α-SMA, un marcador ben establert d'activació de HSCs durant la fibrogènesi hepàtica.

4. El SC-236 redueix els nivells hepàtics de la 15-deoxi-$\Delta^{12,14}$prostaglandina J_2 (15d-PGJ_2) i recupera l'expressió del RNA missatger del PPARγ en fetges de rates tractades amb CCl_4.

En els fetges de rates tractades amb CCl_4 els nivells de la 15d-PGJ_2, el producte de la deshidratació de la PG majoritària hepàtica, la PGD_2, van ser incrementats marcadament mentre que el mRNA del PPARγ, determinat per transcripció reversa i PCR quantitativa a temps real, va ser reduït significativament. Interessantment, el SC-236 va normalitzar els nivells de la 15d-PGJ_2 i va recuperar l'expressió hepàtica del PPARγ.

5. El SC-236 redueix el creixement cel·lular i indueix apoptosi en HSCs i KCs.

Per tal de caracteritzar els mecanismes cel·lulars que es desencadenen dels efectes antifibròtics del SC-236, vam realitzar estudis addicionals amb HSCs i KCs. Les HSCs són el principal tipus cel·lular responsable de la fibrogènesi hepàtica mentre que les KCs són les principals responsables de la inducció de COX-2 i de la biosíntesi d'eicosanoids en el fetge. El SC-236 va reduir de manera temps i concentració depenent la proliferació de les HSCs, un efecte que es va associar amb un increment del número de nuclis amb cromatina densament compactada, característica principal de les cèl·lules apoptòtiques. Es van observar resultats semblants amb KCs. L'efecte del SC-236 en la proliferació de les HSCs va ser semblant al reportat anteriorment pels lligants del PPARγ. De fet, en HSCs, el SC-236 va inhibir la resposta proliferativa induïda per PDGF a una extensió semblant a l'exercida pel lligant del PPARγ rosiglitazone.

6. El SC-236 incrementa l'expressió del mRNA del PPARγ en HSCs i activa el PPARγ en un assaig de transactivació en base cel·lular.

Vam estudiar l'efecte de concentracions creixents de SC-236 sobre l'expressió del PPARγ en HSCs per transcripció reversa i PCR quantitativa a temps real, i vam trobar que el SC-236 incrementava significativament els nivells de mRNA del PPARγ en aquestes cèl·lules. Finalment vam explorar si de la mateixa manera que altres compostos antiinflamatoris i antifibròtics, el SC-236 era capaç d'unir i activar el PPARγ. Per tal d'evitar la interferència del receptor endogen, vam utilitzar un assaig reporter amb base cel·lular del PPARγ i co-transfecció amb la luciferasa. En aquest assaig, el SC-236 va actuar com a agonista del PPARγ de manera concentració depenent. Aquest efecte va ser molt potent i comparable a la inducció exercida

per la 15d-PGJ_2, el lligant natural i activador del PPARγ. En conjunt, aquests resultats suggereixen que l'efecte antifibròtic exercit pel SC-236 en rates tractades amb CCl_4 és mitjançat, almenys en part, per l'activació del PPARγ.

The selective cyclooxygenase-2 inhibitor SC-236 reduces liver fibrosis by mechanisms involving non-parenchymal cell apoptosis and PPARγ activation

Anna Planagumà,* Joan Clària,*,[1] Rosa Miquel,[†] Marta López-Parra,* Esther Titos,* Jaime L. Masferrer,* Vicente Arroyo,[‡] and Joan Rodés[‡]

*DNA Unit, [†]Pathology Laboratory and [‡]Liver Unit, Hospital Clínic, Institut d'Investigacions Biomèdiques August Pi i Sunyer (IDIBAPS), Universitat de Barcelona, Barcelona, Spain

To read the full text of this article, go to http://www.fasebj.org/cgi/doi/10.1096/fj.04-2753fje; doi: 10.1096/fj.04-2753fje

SPECIFIC AIMS

There is growing recognition of the importance of inflammation in initiating the sequence of events leading to liver fibrosis. We have examined the effects of SC-236, a selective cyclooxygenase (COX)-2 inhibitor in experimental liver fibrosis. The investigation is comprised of in vivo studies of rats with carbon tetrachloride (CCl_4)-induced liver injury as well as in vitro studies of Kupffer cells and hepatic stellate cells (HSCs), the major players in liver inflammation and liver fibrogenesis, respectively.

PRINCIPAL FINDINGS

1. COX-2 protein expression is markedly increased in the liver of CCl_4-treated rats

Compared with controls, a marked induction of COX-2 protein expression was detected by immunohistochemistry in the liver of CCl_4-treated rats.

2. The selective COX-2 inhibitor SC-236 reduces liver fibrosis in CCl_4-treated rats

After CCl_4 administration, rats developed hepatic steatosis, inflammation, hepatocyte ballooning, and necrosis. Beyond the 6th wk of CCl_4 treatment, liver architecture was extensively disorganized as the sinusoids were no longer distinguishable; few areas of healthy hepatocytes were present and collagen deposition with septa bridging portal regions was detected. As shown in **Fig. 1*A***, administration of SC-236 to CCl_4-treated rats exerted a significant antifibrotic effect, as revealed by the histological analysis of liver sections and the presence of a lower hepatic hydroxyproline content (13.0 ± 1.4 vs. 16.9 ± 1.4 nmol/mg liver tissue, $P<0.05$), an established marker of collagen synthesis.

3. SC-236 decreases matrix metalloproteinase (MMP)-2 and MMP-9 activities and α-smooth muscle actin (α-SMA) protein expression

Since MMPs are key enzymes in the regulation of extracellular matrix remodeling and their activity closely correlates with the severity of liver fibrosis, we determined hepatic MMP-2 and MMP-9 activities by zymography. SC-236 significantly reduced hepatic MMP-2 gelatinolytic activity and abolished MMP-9 activity in CCl_4-treated rats (Fig. 1*B*). SC-236 dramatically suppressed α-SMA protein expression, a well-established marker of HSC activation during liver fibrogenesis (Fig. 1*C*).

4. SC-236 reduces hepatic levels of 15-deoxy-$\Delta^{12,14}$ prostaglandin (PG) J_2 (15d-PGJ_2) and restores peroxisome proliferator-activated receptor (PPAR) γ mRNA expression in the liver of CCl_4-treated rats

Levels of 15d-PGJ_2, the dehydration product of the major hepatic PG, PGD_2, were markedly increased whereas PPARγ mRNA, as determined by reverse transcription real-time quantitative PCR, was significantly abrogated in the liver of CCl_4-treated rats. SC-236 normalized 15d-PGJ_2 levels and restored PPARγ expression in the liver.

5. SC-236 reduces cell growth and induces apoptosis in HSCs and Kupffer cells

To characterize the cellular mechanisms underlying the hepatic antifibrotic effects of SC-236, we performed additional studies in HSCs and Kupffer cells. HSCs are the major cell type involved in liver fibrogenesis; Kupffer cells are primarily responsible for COX-2 induction and eicosanoid biosynthesis in the liver. As shown in **Fig. 2*A*, *B***, SC-236 reduced, in a concentration- and time-dependent manner, HSC proliferation,

[1] Correspondence: DNA Unit, Hospital Clínic, Villarroel 170, Barcelona 08036, Spain. E-mail: jclaria@clinic.ub.es

0892-6638/05/0019-1120 © FASEB

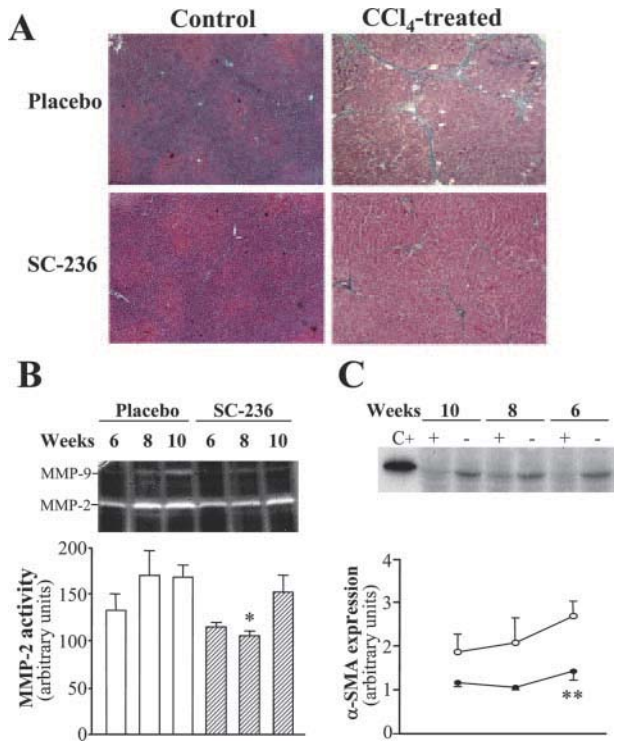

Figure 1. Antifibrotic effects of SC-236 in CCl_4-treated rats. *A)* Histological assessment of liver fibrosis in CCl_4-treated and control rats. The extent of matrix deposition was measured by Masson's trichrome staining of liver tissue sections from control animals (left panels, magnification ×40) and 10 wk CCl_4-treated rats (right panels, ×100) receiving either placebo (upper panels) or SC-236 (lower panels). Data are representative of results obtained from 10 control and 20 CCl_4-treated rats. *B)* Detection of hepatic MMP-2 and MMP-9 activities by zymography. Gelatin polyacrylamide gel representative of changes in activity of MMP-2 (72 kDa) and MMP-9 (92 kDa) during the weeks of CCl_4 administration (6, 8, and 10 wk) in CCl_4-treated rats receiving placebo or SC-236. Lower panel: analysis by densitometry of MMP-2 activity in these samples. The results are the mean ± SE of 5 different experiments. $^*P < 0.05$ vs. placebo. *C)* Effects of SC-236 on hepatic α-SMA protein expression in CCl_4-treated rats. Liver tissue samples from rats with CCl_4-induced fibrosis treated with (+) or without (–) SC-236 were analyzed by Western blot using a specific antibody against α-SMA. A representative blot is shown in the upper panel; the histogram in the lower panel shows the results obtained from the densitometric analysis of band intensities from 4 separate experiments (mean±SE). ○, placebo; ●, SC-236; CT+, total protein from mesangial cells. $^{**}P < 0.01$ vs. placebo.

an effect associated with an increased number of nuclei with densely compacted chromatin characteristic of apoptotic cells (Fig. 2*C*). Similar findings were observed in Kupffer cells. The effect of SC-236 on HSC proliferation was similar to that previously reported for PPARγ ligands. In HSCs, SC-236 inhibited the proliferative response induced by PDGF to an extent similar to that of the PPARγ ligand rosiglitazone.

6. SC-236 increases PPARγ mRNA expression in HSCs and activates PPARγ in a cell-based trans-activation assay

We assessed the effect of increasing concentrations of SC-236 on PPARγ expression in HSCs by reverse transcription and real-time quantitative PCR, and found that SC-236 significantly increases PPARγ mRNA levels in these cells. We explored whether SC-236 is able to bind and activate PPARγ. To avoid interference from the endogenous receptor, we used a cell-based PPARγ and luciferase cotransfection reporter assay. SC-236 acted in a concentration-dependent manner as a PPARγ agonist. This effect was very potent and comparable to the induction exerted by 15d-PGJ_2, the natural ligand and activator of PPARγ. These findings suggest that the antifibrotic effect exerted by SC-236 in CCl_4-treated rats is mediated at least in part by PPARγ activation.

CONCLUSIONS AND SIGNIFICANCE

Inflammation plays a major role in the pathogenesis of liver fibrosis and precedes or coexists with the development of extracellular matrix alterations in this organ. Several anti-inflammatory strategies aimed to efficiently prevent liver fibrosis have been tested. Unfortunately, anti-inflammatory therapies such as glucocorticoids and nonsteroidal anti-inflammatory drugs (NSAIDs) have not proved consistently effective and are not devoid of side effects (i.e., NSAIDs are not recommended in patients with chronic liver disease because of renal side effects). Therefore, novel therapeutic approaches are needed.

A novel strategy to treat liver inflammation and related hepatic disorders may involve the use of selective COX-2 inhibitors. This new class of anti-inflammatory compounds has an efficacy similar to traditional NSAIDs but

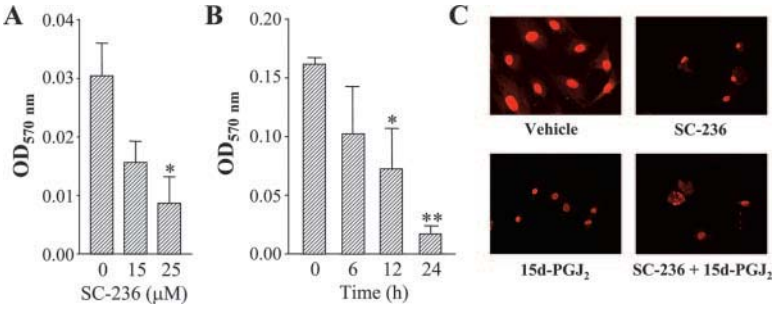

Figure 2. Effects of SC-236 on HSC growth and survival. Concentration and time responses to SC-236. HSCs were incubated with increasing concentrations of SC-236 (0, 15, and 25 μM) for 24 h (*A*) or grown for 0, 6, 12, and 24 h with 15 μM SC-236 (*B*); cell number was determined by the MTT assay. Results are mean ± SE of 3 different experiments with duplicate determinations. $^*P < 0.05$, $^{**}P < 0.01$ vs. untreated cells. *C)* Changes in nuclear morphology associated with programmed cell death were assessed by fluorescence microscopy in HSCs stained with propidium iodide after 6 h of incubation at 37°C with vehicle (0.1% ethanol), SC-236 (25 μM), and 15d-PGJ_2 (10 μM) alone or in combination with SC-236 (25 μM).

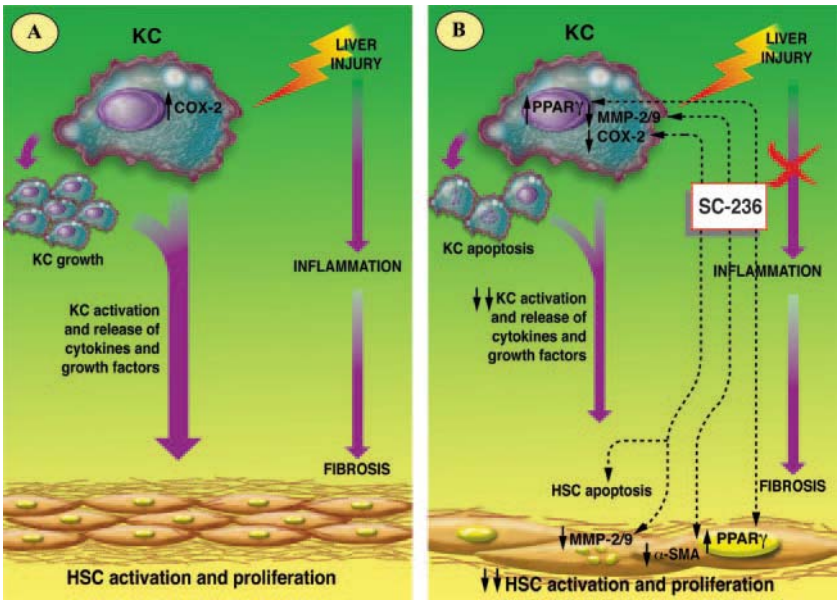

Figure 3. Summary of the proposed mechanism by which SC-236 attenuates liver fibrosis. *A)* Liver injury induces COX-2 overexpression in Kupffer cells (KC) and initiates a cascade of events, including massive production of cytokines and growth factors, leading to hepatic stellate cell (HSC) activation and proliferation, and consequently to liver fibrosis. During fibrosis progression, KC proliferate, thereby amplifying the release of proinflammatory mediators. *B*) The selective COX-2 inhibitor dampens liver inflammation and fibrosis by mechanisms involving PPARγ activation, down-regulation of α-SMA expression and MMP-2 and -9 activities and induction of KC and HSC apoptosis.

with a lower incidence of adverse gastrointestinal and renal effects. In the current study, we provide evidence that the selective COX-2 inhibitor, SC-236, exerts a significant antifibrotic effect in rats with CCl_4-induced liver fibrosis. Our results open new avenues for the applicability of these anti-inflammatory compounds as a novel therapy for liver inflammation and fibrosis. Such a strategy has been shown to be effective in preventing other fibrotic disorders, including renal interstitial fibrosis, fibrosis of the testes, and oral submucous fibrosis.

Our study also provides molecular mechanisms for the antifibrotic effects of SC-236 in the liver of CCl_4-treated animals. Our results support the concept that the antifibrogenic effects of SC-236 are mediated at least in part by PPARγ (**Fig. 3**). In fact, SC-236 increased PPARγ expression in HSCs and restored its expression to normal levels in the liver of CCl_4-treated rats. PPARγ is a ligand-activated transcription factor with a DNA binding domain that recognizes response elements in the promoter region of specific target genes linked to inflammation, cell proliferation, apoptosis, and differentiation. PPARγ plays a pivotal role in the progression of liver fibrosis since HSC activation is associated with a reduction in both expression and transcriptional activity of this nuclear receptor. In culture-activated HSCs, synthetic PPARγ ligands restore PPARγ and reverse the activated HSCs to the quiescent phenotype. In vivo, administration of synthetic PPARγ ligands (i.e., antidiabetic thiazolidinediones) to animal models of liver fibrosis effectively reduces HSC trans-differentiation and collagen deposition. The results obtained in our trans-activation reporter assay are indicative that SC-236 not only restores PPARγ expression, but also works as a PPARγ ligand. This effect was very potent and comparable to the induction exerted by 15d-PGJ_2, the natural ligand and activator of PPARγ. These findings together with the observation that the antiproliferative effects of SC-236 were similar to those exerted by the PPARγ ligand rosiglitazone support the concept that the antifibrotic properties of SC-236 are related to PPARγ.

The results of our study also indicate that SC-236 exhibits proapoptotic and growth-inhibitory properties in HSCs and Kupffer cells (Fig. 3). Identification of SC-236 as an apoptotic stimulus for nonparenchymal liver cells may have pathophysiological implications. Activated HSCs are central to liver fibrosis as the major source of collagens I and III. During fibrotic injury, these retinoid-rich, nonparenchymal cells proliferate and undergo a phenotypic transformation to myofibroblast-like cells, a process termed activation. Therefore, the control of HSC proliferation and apoptosis is a key event in regulating the progression of liver fibrosis. Strategies based on inhibition of HSC proliferation and induction of HSC apoptosis have proved to be potential antifibrotic approaches. On the other hand, Kupffer cells, the resident macrophages of the liver, are well recognized for their activity in liver inflammation and to promote activation of HSCs through release of paracrine factors. The presence of an increased number of activated Kupffer cells is considered to be critical in the initiation of the inflammatory cascade leading to liver fibrosis. Consistent with their role in liver inflammation, selective depletion of macrophages during progression of injury or reduction of Kupffer cell survival by inhibition of the 5-lipoxygenase pathway are associated with a remarkable antifibrotic effect. Results of the current study suggest that inhibition of Kupffer cell survival by SC-236 contributes to the dampening of liver fibrogenesis. Although we did not establish the exact mechanisms underlying the proapoptotic properties of SC-236, several molecular mechanisms, including COX-dependent and COX-independent pathways, are likely to be implicated.

The results of the current study bring to light the antifibrogenic potential of the selective COX-2 inhibitor SC-236 and open new avenues for the development of novel anti-inflammatory strategies leading to an effective therapy for liver fibrosis. FJ

The FASEB Journal express article 10.1096/fj.04-2753fje. Published online May 4, 2005.

The selective cyclooxygenase-2 inhibitor SC-236 reduces liver fibrosis by mechanisms involving non-parenchymal cell apoptosis and PPARγ activation

Anna Planagumà,* Joan Clària,* Rosa Miquel,† Marta López-Parra,* Esther Titos,* Jaime L. Masferrer,* Vicente Arroyo,‡ and Joan Rodés‡

*DNA Unit, †Pathology Laboratory, and ‡Liver Unit, Hospital Clínic, Institut d´Investigacions Biomèdiques August Pi i Sunyer (IDIBAPS), Universitat de Barcelona, Barcelona, Spain

Corresponding author: Joan Clària, DNA Unit, Hospital Clínic, Villarroel 170, Barcelona 08036, Spain. E-mail: jclaria@clinic.ub.es

ABSTRACT

The importance of inflammation in initiating the sequence of events that lead to liver fibrosis is increasingly recognized. In this study, we tested the effects of SC-236, a selective cyclooxygenase (COX)-2 inhibitor, in rats with carbon tetrachloride (CCl_4)-induced liver fibrosis. Livers from CCl_4-treated rats showed increased COX-2 expression and 15-deoxy-prostaglandin (PG)J_2 (15d-PGJ_2) formation, as well as decreased peroxisome proliferator-activated receptor (PPAR)γ expression. In these animals, SC-236 reduced liver fibrosis as revealed by histological analysis and by a reduction in hepatic hydroxyproline levels, metalloproteinase-2 activity, and α-smooth muscle actin expression. Interestingly, SC-236 normalized 15d-PGJ_2 levels and restored PPARγ expression in the liver of CCl_4-treated rats. In isolated hepatic stellate cells (HSCs)—the major player in liver fibrogenesis—and Kupffer cells—the cell type primarily responsible for increased hepatic COX-2—SC-236 exhibited remarkable pro-apoptotic and growth inhibitory properties. Of interest, SC-236 decreased HSC viability to a similar extent than the PPARγ ligand rosiglitazone. Moreover, SC-236 significantly induced PPARγ expression in HSCs and acted as a potent PPARγ agonist in a luciferase-reporter trans-activation assay. These data indicate that, by mechanisms involving non-parenchymal cell apoptosis and PPARγ activation, the selective COX-2 inhibitor SC-236 might have therapeutic potential for prevention of liver fibrosis.

Key words: inflammation • liver injury • Kupffer cells • hepatic stellate cells • nuclear receptors

Liver fibrosis is the accumulation of connective tissue in the liver as the result of an imbalance between production and degradation of extracellular matrix (1, 2). Over the past few years, we have witnessed a remarkable advancement in the knowledge of the cellular and molecular mechanisms underlying this liver complication. These investigations have led to the concept that inflammation is a key component of the etiology of liver fibrosis because it precedes or coexists with the development of hepatic extracellular matrix alterations (1, 2).

Because inflammation is histologically present in virtually all forms of liver fibrosis, several anti-inflammatory strategies have been tested to efficiently prevent hepatic fibrogenesis. Glucocorticoids and colchicine, for example, are representative anti-inflammatory agents of potential therapeutic use in alcoholic hepatitis, although the efficacy of these drugs remains of unproven value as anti-fibrotic agents (3). However, nonsteroidal anti-inflammatory drugs (NSAIDs) appear to be useful in preventing the development of experimental liver fibrosis, cirrhosis, and hepatic focal lesions caused by a choline-deficient diet (4). Unfortunately, these drugs are not recommended in patients with liver disease because of renal side effects (5). Therefore, because the lack of specificity and the adverse effects of these anti-inflammatory therapies represent an important limitation, at present, an effective anti-inflammatory strategy that prevents the progression or even reverses established fibrosis still remains elusive.

Cyclooxygenase (COX)-2 is a key executor of uncontrolled inflammation (6, 7). COX-2 is an inducible immediate-early gene originally identified to be up-regulated by several pro-inflammatory stimuli, including cytokines, mitogens, and growth factors (6, 7). Over-expression of COX-2 has been reported in several chronic inflammatory diseases such as rheumathoid arthritis, Crohn's disease, and ulcerative colitis (6, 7). Regarding the liver, up-regulation of COX-2 has been demonstrated in human cirrhosis as the result of active inflammation (8, 9). In addition, COX-2 is associated with progressive hepatic fibrosis in chronic hepatitis C infection (10). COX-2 has also been shown to be up-regulated in the context of necroinflammatory injury in rats with experimental alcoholic liver disease and rats submitted to a choline-deficient, L-amino acid-defined diet (11–13). These findings indicate that COX-2 is an appealing target in the liver and, consequently, the recently developed selective COX-2 inhibitors may represent a novel therapeutic strategy to prevent liver fibrosis. In fact, selective COX-2 inhibitors are effective in the prevention of fibrotic disorders, including renal interstitial fibrosis, fibrosis of the testes, and oral submucous fibrosis (14–16). Given that the applicability of clinically available selective COX-2 inhibitors to the prevention of liver fibrogenesis has not been explored, the current study was aimed to evaluate the effects of SC-236, a selective COX-2 inhibitor, on experimental liver fibrosis.

MATERIAL AND METHODS

Animals and experimental design

All animal studies were conducted in accordance with the criteria of the Investigation and Ethics Committee of the Hospital Clínic and the European Community laws governing the use of experimental animals. Seventy-six male adult Wistar rats weighing 200–220 g were included in the fibrosis induction program by inhalation of carbon tetrachloride (CCl_4) (twice weekly, Mondays and Fridays). Animals were fed ad libitum with standard chow and distilled water containing phenobarbital (0.3 g/l) as drinking fluid. The experimental study comprised two different drug regimens. In the first regimen (Study A), animals included in the CCl_4-induction program were randomly assigned to receive by gavage either the selective COX-2 inhibitor SC-236 (6 mg/kg b.w. weekly; n=30), starting with an initial dose of 12 mg/kg b.w. 1 week before the first administration of CCl_4 or placebo (0.5% carboxymethylcellulose, n=30) (Fig. 1). Two groups of control animals (rats not submitted to the CCl_4 fibrosis-induction program), receiving either SC-236 (n=15) or placebo (n=15), were also included in Study A. The second drug regimen (Study B) consisted in giving SC-236 (6 mg/kg b.w. by gavage) three times per week

starting 1 week before the administration of CCl_4 or placebo (0.5% carboxymethylcellulose) to 16 male Wistar rats submitted to CCl_4-induced fibrosis. In both regimens, animals were sacrificed in a staggered fashion under ketamine anesthesia at the 6th, 8th, and 10th week of the fibrosis induction program (Fig. 1). After animal sacrifice, specimens of liver tissue were obtained and fixed in either 4% formalin for histological analysis or molecular biology fixative (MBF) for immunohistochemistry studies. Portions of liver tissue were also snap-frozen in liquid nitrogen for further RNA and protein analysis and biochemistry measurements.

Immunohistochemical analysis of COX-2 protein expression in the liver

COX-2 protein expression was assessed in liver tissue from CCl_4-treated and control rats. Following sacrifice, livers were rapidly resected and cut to the appropriate size to facilitate efficient fixative penetration of MBF. MBF is an aqueous buffered solution containing organic and inorganic salts and supplemented with a bacteriostatic and fungistatic agent that provides excellent preservation of tissue structure and COX antigenicity. Tissues were fixed for 24 h at 4°C, transferred to 70% ethanol, embedded in paraffin, sectioned at 5 µm onto glass slides, and finally deparaffinized in xylene and re-hydrated in descending alcohols. Tissues were then blocked for endogenous peroxidase (3% H_2O_2 in MeOH) and avidin/biotin (Avidin Biotin Blocking Kit SP-2001). Sections were permeabilized in TNB-BB (0.1 M Tris, pH 7.5, 0.015 M NaCl, 0.5% blocking agent, 0.3% Triton-X and 0.2% saponin) and were incubated overnight at 4°C with polyclonal rabbit anti-murine COX-2 serum diluted to 2.5 µg/ml. Immunoreactive complexes were detected using a tyramide signal amplification kit and visualized with the peroxidase substrate 3-amino-9-ethyl-carbazole (AEC). Control slides were treated with either no primary antibody or with isotype-matched IgG serum. Specificity for COX-2 was confirmed by preincubating COX-2 antibody with 100X recombinant COX-2 protein prior to addition to the slides.

Liver histology

Formalin-fixed sections (5 µm) of the right and left liver lobes were stained with hematoxylin and eosin and Masson's trichrome, coded for blind analysis, and scored by a registered pathologist unaware of the treatments as follows. Stage 0: Absent. Normal lobular architecture. Stage 1: Pericentral fibrosis (increased thickness of the central vein). Stage 2: Central anastomoses (some fibrous septa connecting central veins). Stage 3: Pre-cirrhotic stage (fibrous septa with marked distorsion of the liver lobules). Stage 4: Cirrhosis (nodule regeneration surrounded by broad connective tissue septa).

Hepatic concentration of hydroxyproline

Hydroxyproline concentration, an index of collagen content, was determined by reverse-phase (RP)-HPLC (17). Briefly, liver slices of approximately 40 mg were hydrolyzed in 6N HCl at 110°C for 18 h. Hydroxyproline concentration was measured after its derivatization with phenylisothiocyanate. The phenylthiocarbamyl hydroxyproline derivative was injected into a C_{18} column using an isocratic solvent of sodium acetate (pH 4.6) for 10 min at a flow rate of 1 ml/min.

Analysis of metalloproteinase (MMP)-2 and 9 activities by gelatin zymography

Liver samples were homogenized at 4ºC in a 50 mM Tris-HCl (pH 7.5) containing 0.15 mM NaCl, 10 mM $CaCl_2$, 1 μg/ml aprotinin, 10 μg/ml leupeptin, and 10 μg/ml pepstatin. The homogenates were centrifuged at 10000 *g* for 20 min at 4ºC, the supernatants collected and the protein content was determined by the Bradford assay. Proteins were analyzed for gelatinolytic activity by gelatin zymography. Briefly, supernatants from liver homogenates (50 μg of protein) were subjected to 7% SDS-PAGE using 0.13% gelatin-containing gels. After electrophoresis, gels were washed twice for 15 min in 2.5% Triton X-100 to remove the SDS and were incubated at 37ºC during 22 h in 5 mM $CaCl_2$, 50 mM Tris-HCl (pH 8.0), 0.02% NaN_3, and 2 μM ZnCl. Gels were subsequently stained in Coomassie blue and destained in equilibrated buffer (3% glycerol, 10% acetic acid and 40% methanol). Bands of 62, 72, and 92 kDa, which correspond to the active and latent forms of MMP-2 and to the active form of MMP-9, respectively, were scanned and the activities in the gel slabs were quantified using an image analysis program (Phoretix software).

Analysis of α-smooth muscle actin (α-SMA) protein expression

Total liver tissue protein was extracted in lysis buffer containing 20 mM Tris-HCl, pH 7.4, 1% Triton X-100, 10% glycerol, 137 mM NaCl, 2 mM EDTA, and protease inhibitors [PMSF (100 μM) and leupeptin, pepstatin A, and aprotinin, 1 μg/ml each]. Thereafter, the lysate was centrifuged at 3000 *g* for 5 min, the supernatant was collected, and total protein concentration was determined by the MicroBCA™ protein assay. Aliquots from each sample containing equal amounts of protein (10 μg) were resuspended in SDS-containing Laemmli sample buffer, heated at 100ºC for 5 min, electrophoresed on 10% SDS-PAGE, and transferred overnight to polyvinylidene difluoride membranes. Gels were stained with Coomassie to visualize loading differences and membranes submitted to Ponceau S staining to monitor the efficiency of the transfer. The blots were subsequently blocked for 1 h in Tris-buffered saline (TBS: 20 mM Tris-HCl, pH 7.4, and 0.5 M NaCl) containing 5% nonfat dry milk and 0.5% Tween 20, followed by incubation for 2 h with a mouse monoclonal antibody specific for α-SMA (1:5000 dilution). After being washed three times for 5 min each with 0.1% Tween 20 in TBS, the blots were incubated for 1 h at room temperature with a sheep anti-mouse secondary antibody conjugated to horseradish peroxidase (1:10000 dilution). The blots were finally washed as previously described and bands visualized by an enhanced chemiluminescence detection system.

Analysis of peroxisome proliferator-activated receptor (PPAR) γ mRNA expression by reverse transcription and real-time quantitative PCR

Total RNA was extracted with Trizol reagent according to the manufacturer's instructions. RNA concentration was assessed in a UV-spectrophotometer and its integrity tested on a 6000 LabChip in a 2100 Bioanalyzer (Agilent Technologies, Palo Alto, CA). First-strand cDNA was generated from 1 μg of total RNA with an AMV reverse-transcriptase system. Real-time quantitative PCR was performed with an ABI Prism 7900 Sequence Detection System (Applied Biosytems, Foster City, CA) using the fluorescent Taqman methodology. A ready-to-use primer and probe set pre-designed by Applied Biosystems (Assay-on-demand Gene Expression Product Number Rn00440945_m1, Pparg) was used for the detection of rat PPARγ. A primer and probe set for rat β-actin mRNA was used for normalization (Assay-on-demand Gene Expression

Product Number Rn00667869_m1, Actb). The thermal cycling conditions comprised 2 min at 50ºC, 10 min at 95ºC, and 40 cycles of 15 sec denaturation at 95ºC, and 60 sec annealing/extension at 60ºC. Relative quantitation was accomplished by calculating the cycle threshold (C_t), the PCR cycle at which the fluorescence arises above the background signal. The ratio between the C_t value for PPARγ and the respective C_t value for β-actin was then calculated, and the quantity of target messenger was obtained from a standard curve.

Measurement of 15-deoxy-$\Delta^{12,14}$PGJ$_2$ (15d-PGJ$_2$) by enzyme immunoassay (EIA)

Liver tissue samples were homogenized in 0.1 M phosphate buffer, acidified to pH ~3.5, transferred into a syringe, and loaded onto C_{18}-silica reverse-phase cartridges. Ethyl acetate-eluted materials were concentrated under a stream of N_2 and 15d-PGJ$_2$ levels determined by a highly specific EIA.

PPARγ transactivation assay

A fusion protein containing the yeast GAL4 DNA-binding domain linked to the ligand-binding domain of PPARγ (PPARγ-GAL4 plasmid) and a luciferase reporter construct containing four copies of a GAL4 upstream activating sequence (UAS_G) and a thymidine kinase (tk) promoter (MH100-tk-luc plasmid) were kindly provided by R. Evans (Salk Institute, La Jolla, CA). This chimeric PPARγ activates transcription through a heterologous response element and allows PPARγ activity to be assayed independently of endogenous receptors (18).

To determine the ability of SC-236 to activate PPARγ, COS 7 cells (1.5×10^4 cells/well) were plated in 12-well plates at 70% confluence and co-transfected with 1 ml of DMEM containing 0.3 μg of the luciferase reporter construct MH100-tk-luc, 0.1 μg of PPARγ-GAL4, and 0.002 μg of β-gal expression vector pCMV (an internal control plasmid containing a cytomegalovirus promoter) by using the Effectene® transfection reagent at a ratio of 1:10 to DNA, according to the manufacturer's instructions. Thirty hours after transfection, the medium was removed from cells and washed twice with DPBS with Ca^{++} and Mg^{++} before addition of vehicle (0.5% ethanol), increasing concentrations of 15d-PGJ$_2$ (1, 3, and 10 μM) and SC-236 (3 and 10 μM) alone or in combination with 15d-PGJ$_2$ (1 μM) for 18 h. At the end of the incubation, cells were harvested in luciferase lysis buffer, and light units from firefly luciferase and β-gal activities were measured in a Lumat LB 9507 luminometer (Berthold, Bad Wildbad, Germany). Luciferase values were expressed as relative light units (RLU) and normalized to the level of β-gal activity. Changes in PPARγ activity were expressed as "fold induction" relative to the vehicle control values.

To determine the capacity of hepatic lipid extracts to activate PPARγ, lipid components from liver tissue were extracted according to the two-step Bligh and Dyer method (19). Briefly, liver samples (0.2–0.5 g) were homogenized in 1 ml Tris/HCl (30 mM pH 7.4), followed by the addition of 3.75 ml of chloroform/methanol (1:2, v/v), and mixed for 10 min. Subsequently, chloroform (1.25 ml) was added and mixed for 1 min followed by water (1.25 ml) and mixing for another minute. Samples were then left standing for 30 min at room temperature, and the lower organic phase was collected. Thereafter, chloroform (1.88 ml) was added to the remaining aqueous phase residue, mixed, and centrifuged at 800 *g* for 5 min at room temperature. The

lower phase was again collected, pooled with the first organic phase, and dried under a N_2 stream. After evaporation, the lipid extract was dissolved in methanol-water (1:45, v/v), transferred into a syringe, acidified to pH 3.5, and loaded onto C_{18}-silica reverse-phase cartridges. Materials were eluted from the cartridge with hexane, concentrated under a stream of N_2, resuspended in DMSO, and tested in the trans-activation assay.

Kupffer cell isolation and culture

Male wistar Rats weighing 200–300 g were anesthetized with ketamine (50 mg/kg b.w.) and liver cells were isolated by in situ collagenase perfusion through the portal vein as described elsewhere (20, 21). Briefly, livers were perfused for 20 min at a flow rate of 14 ml/min at 37°C with HBSS without calcium and magnesium containing 10 mmol/L HEPES (pH 7.4) and 1 mmol/L EGTA, followed by 5 min with HBSS containing 10 mmol/L HEPES (pH 7.4), 1.3 mmol/L $CaCl_2$ and 0.6% BSA, and then 10 min with a 0.05% collagenase (A type) solution containing 10 mmol/L HEPES (pH 7.4) and 1.3 mmol/L $CaCl_2$. The resultant digested liver was excised and minced, and the dispersed cells were passed through nylon mesh filters (100 µm). The hepatic cell suspension was centrifuged twice at 50 *g* for 5 min, and the supernatant was centrifuged again at 800 *g* for 10 min at 4ºC. The obtained pellet was resuspended in DPBS and centrifuged at 800 *g* for 24 min through a 25%/50% Percoll gradient at 4ºC. The interface of the gradient was seeded on 35-mm tissue culture plates and incubated at 37°C for 30 min. Cell monolayers adhered to the dishes were characterized as Kupffer cells and cultured in RPMI 1640 medium supplemented with 2 mM L-glutamine, penicillin (50 U/ml), streptomycin (50 µg/ml), and 5% FCS in a humidified 5% CO_2 incubator at 37 °C.

Hepatic stellate cell (HSC) isolation and culture

HSCs were isolated from male Wistar rats by in situ perfusion with pronase and collagenase (22). Briefly, livers were perfused through the portal vein for 20 min at a flow rate of 14 ml/min at 37°C with HBSS without calcium and magnesium, followed by 10 min with Gey's balanced salt solution (GBSS) containing 0.003% DNase, 0.02% collagenase (A type), and 0.2% pronase. The resultant digested liver was excised and minced and shaked at 37ºC for 10 min with GBSS containing 0.003% DNase, 0.006% collagenase, and 0.02% pronase, and the dispersed cells passed through nylon mesh filters (100 µm). The hepatic cell suspension was centrifuged 1000 *g* for 10 min at room temperature and the pellet was resuspended in GBSS and centrifuged again at 1000 *g* for 10 min at room temperature. The obtained pellet was resuspended in GBSS, centrifuged at 1000 *g* for 15 min through a 13% Nycodenz gradient at room temperature. The interface of the gradient was seeded on 35-mm tissue culture plates and incubated at 37°C in Iscove's modified Dulbecco's medium supplemented with 10% FCS, 2 mM L-glutamine, penicillin (50 U/ml), streptomycin (50 µg/ml), insulin (100 IU/ml), 0.1 mM non-essential amino acids, and 0.1 mM sodium pyruvate in a humidified 5% CO_2 incubator at 37°C. Experiments were performed after the first serial passage when cells already showed morphological features of culture-activated HSCs.

Cell growth assay

To ascertain the effects of SC-236 on cell growth, rat macrophages (CRL-2192, 1×10^5 cells/well) and HSCs (5×10^4 cells/well) were seeded in 24-well plates in 1 ml of complete RPMI 1640

medium and Iscove's modified Dulbecco's medium, respectively, at 37°C in a 5% CO_2 atmosphere. Cells were serum-deprived for 1 h and incubated in serum-free media in the presence of vehicle (0.5% ethanol) or increasing concentrations of SC-236 (10, 15, and 25 μM) for 6–24 h at 37ºC. In some experiments, HSCs were serum-deprived and pre-incubated with SC-236 (10 and 25 μM), rosiglitazone (5 μM), or vehicle for 15 min and then exposed to PDGF (50 ng/ml) for 18 h at 37ºC. Cell growth was determined by adding 20 μl of MTT (5 mg/ml) to each well for 4 h and subsequent lysis of the cells with 200 μl of isoamyl alcohol and shaking for 20 min. The absorbance at 570 nm was measured in a multi-well plate reader (Molecular Devices, Menlo Park, CA).

Apoptosis assays

Changes in nuclear morphology were assessed by fluorescence microscopy in Kupffer cells and HSCs growing in 8-well Lab-Tek® Chamber Slides™ in RPMI 1640 medium and Iscove's modified Dulbecco's medium, respectively. Cells were exposed to vehicle (0.1% ethanol), 1% ethanol, increasing concentrations of SC-236 (25 and 50 μM), and 15d-PGJ_2 (10 μM) alone or in combination with SC-236 (25 μM) for 6 h, and thereafter washed twice with DPBS and fixed with 3% formaldehyde for 20 min at room temperature. Following a further fixation and permeabilization in ice-cold 100% methanol for 20 min, cells were gently washed three times and then stained for 10 min with 50 μg/ml propidium iodide in a DPBS solution containing 200 μg/ml RNase A. Coverslips were mounted and nuclei morphology was analyzed by fluorescence microscopy. Apoptosis was also assessed in CRL-2192 cells growing in 8-well Lab-Tek® Chamber Slides™ in RPMI 1640 medium and exposed to vehicle (0.1% ethanol), gadolinium chloride (270 μM), SC-236 (25 and 50 μM), and 15d-PGJ_2 (10 μM) alone or in combination with SC-236 (25 μM), as described above. Apoptosis in Kupffer and CRL-2192 cells was confirmed by optical microscopy in Diff-Quik®-stained cytospin preparations.

Materials

Animals were from Charles River (Saint Aubin les Elseuf, France). C_{18}-silica columns were purchased from Waters Associates (Milford, MA). Gelatin, MTT, Nycodenz, GBSS, propidium iodide and monoclonal anti-α-SMA (clone 1A4) were from Sigma (St. Louis, MO). Iscove's modified Dulbecco's medium was from Biological Industries (Kibbutz Beit Haemek, Israel). Rosiglitazone was from Cayman (Ann Arbor, MI). The Trizol reagent was from Invitrogen (Carlsbad, CA); 30% acrylamide/bis solution and Bio-Safe™ Coomassie were from Bio-Rad (Hercules, CA). Percoll and the ECL system were from Amersham (Buckinghamshire, UK). Immobilon-P membranes were from Millipore (Bedford, MA). The avidin/biotin blocking kit was from Vector Laboratories (Burlingame, CA). The murine COX-2 antibody was from Oxford Biomedical Research (Oxford, MI). The first-strand cDNA synthesis kit was from Promega (Madison, WI). The PPARγ and β-actin Assays-on-demand were from Applied Biosystems (Foster City, CA). The Lab-Tek® Chamber Slides™ were from Nalge Nunc International (Naperville, IL). Diff-Quik® was from Dade Behring (Düdingen, Switzerland). SC-236 was provided by Pfizer (St. Louis, MO). Collagenase (A type), pronase, DNase, and RNase were from Roche (Basel, Switzerland). The 15d-PGJ_2 EIA kit was from Assay Designs (Ann Arbor, MI).

Statistical analysis of the results was performed using the analysis of variance and the paired and unpaired Student's *t*-test. Results were expressed as mean ± SEM, and differences were considered significant at a $P < 0.05$.

RESULTS

To evaluate the contribution of COX-2 to the pathogenesis of liver fibrosis, the selective COX-2 inhibitor SC-236 was administered to CCl_4-treated and control rats and the effects were compared with those of placebo. Comparable body weight gains were observed throughout the study in all groups of animals (data not shown). A marked induction of COX-2 protein expression was detected by immunohistochemistry in the liver of CCl_4-treated rats (Fig. 2). These animals developed hepatic steatosis, inflammation, hepatocyte ballooning, and necrosis. Beyond the 6th week of CCl_4-treatment, the liver architecture was extensively disorganized, as the sinusoids were no longer distinguishable, and few areas of healthy hepatocytes were present (Fig. 3*A*, upper right panel). The examination of the Masson's trichrome-stained liver sections revealed extensive collagen deposition with septa bridging portal regions (Fig. 3*A*, upper right panel). The administration of SC-236 to CCl_4-treated rats significantly reduced the degree of liver fibrosis (Fig. 3*A*, lower right panel), an inhibitory effect that was more pronounced in the drug regimen of Study B than in that of Study A (Table 1). Interestingly, none of the animals treated with SC-236 for 6 weeks in Study B developed liver fibrosis (Table 1). No histological alterations were observed during the entire study period in control rats treated with placebo or SC-236 (Fig. 3*A*, upper and lower left panels). The anti-fibrotic properties of SC-236 in CCl_4-treated animals were biochemically confirmed by measuring hepatic hydroxyproline content. In both drug regimens (Studies A and B), the hepatic content of this marker of collagen synthesis was significantly lower in CCl_4-treated rats receiving SC-236 than in those receiving placebo (Table 2).

Given that MMPs are key enzymes in the regulation of extracellular matrix remodeling and that their activity closely correlates with the severity of liver fibrosis (23), we next compared MMP-2 and MMP-9 activities in liver tissue samples obtained from CCl_4-treated rats receiving SC-236 with those receiving placebo. As shown in Fig. 3*B*, both the 72 kDa gelatinase A (MMP-2) and the 92 kDa gelatinase B (MMP-9) gelatinolytic activities were detected by zymography in rat liver samples. As compared to placebo, hepatic MMP-2 gelatinolytic activity was decreased in rats treated with the selective COX-2 inhibitor SC-236, an effect that reached statistical significance at the 8th week of SC-236 treatment (Fig. 3*B*). Interestingly, at the 10th week of CCl_4 treatment, MMP-9 activity was completely abolished by SC-236 (Fig. 3*B*).

To provide further evidence of the anti-fibrotic properties of SC-236 in CCl_4-treated animals, we used Western blot analysis to determine the effects of this compound on hepatic α-SMA protein expression, a well-established marker of HSC activation during liver fibrogenesis (1, 2). As shown in Fig. 3*C*, and as compared to placebo, SC-236 dramatically suppressed α-SMA expression in CCl_4-treated rats.

We next analyzed the levels of 15d-PGJ_2, the dehydration product of the major hepatic PG, PGD_2, and the mRNA expression of PPARγ in the liver of control and CCl_4-treated rats receiving either SC-236 or placebo. As compared to control animals, hepatic levels of 15d-PGJ_2 were markedly increased (Fig. 4*A*), whereas PPARγ expression was significantly abrogated (Fig.

4*B*) in CCl_4-treated rats. Interestingly, SC-236 normalized 15d-PGJ_2 levels and restored PPARγ expression in the liver (Fig. 4). Moreover, liver tissue extracts from CCl_4-injured rats treated with SC-236 had a higher PPARγ activity than those receiving placebo (data not shown).

In order to characterize the cellular mechanisms underlying the hepatic anti-fibrotic effects of SC-236, we performed additional studies in isolated non-parenchymal liver cells, namely Kupffer cells and HSCs. We first performed experiments in Kupffer and CRL-2192 cells because cells of the macrophage lineage are responsible for COX-2 induction in pro-inflammatory states and the main source of PGs and other eicosanoids in the liver (12, 24, 25). As shown in Fig. 5*A*, SC-236 strongly inhibited, in a time- and concentration-dependent manner, macrophage viability. Furthermore, the inhibitory actions of SC-236 on macrophage cell number were associated with induction of apoptosis. As shown in Fig. 5*B*, propidium iodide staining of Kupffer cells incubated with increasing concentrations of SC-236 showed an increased number of nuclei with densely compacted chromatin characteristic of apoptotic cells. Ethanol at a concentration of 1%, a well-established inductor of macrophage apoptosis, was used as a positive control (Fig. 5*B*). Moreover, 15d-PGJ_2 elicited potent apoptotic actions in rat Kupffer cells and this cyclopentenone PG further enhanced the apoptotic effect of SC-236 (Fig. 5*B*). Similar changes in cell morphology were observed in CRL-2192 cells (data not shown).

We also assessed the effects of SC-236 on the growth and viability of HSCs, the major cell type involved in liver fibrogenesis (1, 2). Incubation of HSCs with increasing concentrations of SC-236 resulted in a concentration and time-dependent inhibition of HSC proliferation (Fig. 6*A* and *B*). SC-236, either alone or in combination with 15d-PGJ_2, induced a marked pro-apoptotic effect in HSCs in culture (Fig. 6*C*). Moreover, the stimulation of HSC proliferation by PDGF was virtually eliminated by SC-236 at concentrations of 25 μM (Fig. 7). The inhibitory effect of SC-236 on HSC proliferation was similar to that previously reported for PPARγ ligands (26–28). In fact, in HSCs, SC-236 inhibited the proliferative response induced by PDGF to a similar extent that the PPARγ ligand rosiglitazone, although their effects were not synergic (Fig. 7).

To better define the mechanisms of action of SC-236, we evaluated whether this compound modifies PPARγ expression in isolated HSCs. To this end, HSCs were grown in the presence of increasing concentrations of SC-236 and total RNA was extracted and PPARγ expression determined by reverse transcription and real-time quantitative PCR. As shown in Fig. 8*A*, SC-236 significantly increased PPARγ mRNA expression in HSCs. In addition, we explored whether SC-236, similar to other anti-inflammatory and anti-fibrotic compounds (29), can bind and activate PPARγ. In order to avoid the interference from the endogenous receptor, we tested the compounds in a cell-based PPARγ-GAL4 and luciferase co-transfection reporter assay. In this assay, SC-236 acted in a concentration-dependent manner as a PPARγ agonist (Fig. 8*B*). At concentrations of 10 μM, SC-236 increased the activity of this nuclear receptor to a similar extent to that of the natural PPARγ ligand 15d-PGJ_2 (Fig. 8*B*). Furthermore, these two compounds acted synergically in the activation of PPARγ (Fig. 8*B*).

DISCUSSION

Our study provides evidence of the existence of a marked induction of COX-2 expression in livers from CCl_4-treated rats, which is consistent with previous reports showing over-expression

of COX-2 during necro-inflammatory changes in rats with alcoholic liver disease and rats induced to liver fibrosis by a choline-deficient, L-amino acid-defined diet (11–13). In humans, increased levels of COX-2 have been reported in patients with chronic hepatitis and liver cirrhosis (8–10). Current evidence point to Kupffer cells as being the cell type primarily responsible for increased COX-2 in the liver. In fact, these liver resident macrophages are uniquely positioned as the predominant inflammatory effector cells in this organ and possess both COX-2 expression and most of the hepatic capacity to produce arachidonic acid-derived lipid mediators (12, 20, 21, 24, 25, 30). However, the contribution of other non-parenchymal liver cells to COX-2 over-expression in CCl_4-treated livers cannot be completely excluded. For instance, HSCs show COX-2 expression in culture, which is induced during the transition toward an activated phenotype and after stimulation with TNFα, IL-1α or TGF-β1 (31–33).

The selective COX-2 inhibitor, SC-236, exhibited pro-apoptotic and growth inhibitory properties in HSCs and Kupffer cells. These actions were similar to those previously reported in other cell types exposed to SC-236 or celecoxib (34, reviewed in 35). The identification of SC-236 as an apoptotic stimulus for non-parenchymal liver cells may have pathophysiological implications. In this regard, activated HSCs are central to liver fibrosis as the major source of collagens I and III (1, 2). During fibrotic injury, these retinoid-rich non-parenchymal cells proliferate and undergo a phenotypic transformation to myofibroblast-like cells, a process termed "activation". Therefore, the control of HSC proliferation and apoptosis is a key event in regulating the progression of liver fibrosis. Indeed, strategies based on inhibition of HSC proliferation and induction of HSC apoptosis have proven to be potential anti-fibrotic approaches (26, 36, 37). On the other hand, Kupffer cells, the resident macrophages of the liver, are well recognized for their activity in liver inflammation and to promote activation of HSCs through release of paracrine factors (1, 2, 25, 38). Therefore, the presence of an increased number of activated Kupffer cells is considered to be a critical event in the initiation of the inflammatory cascade leading to liver fibrosis (20, 25, 39). Consistent with the role of macrophages in liver inflammation, their selective depletion during progression of injury or reduction of Kupffer cell survival by inhibition of the 5-lipoxygenase pathway is associated with a remarkable anti-fibrotic effect (20, 40). The results of the current study suggest that inhibition of Kupffer cell survival by SC-236 also contributes to dampen liver fibrogenesis. The mechanisms by which SC-236 induces apoptosis are not well defined, but several molecular mechanisms, including COX-dependent [modulation of PG biosynthesis (41)] and COX-independent pathways [regulation of activator protein-1 (42), inhibition of serine/threonine protein kinase B (Akt) phosphorylation (43) and down-regulation of protein kinase C (34)], have been suggested.

A major finding of the current study was that the selective COX-2 inhibitor, SC-236, increased PPARγ expression in HSCs and restored its expression to normal levels in the liver of CCl_4-treated rats. PPARγ is a ligand-activated transcription factor with a DNA binding domain that recognizes response elements in the promoter region of specific target genes linked to inflammation, cell proliferation, apoptosis, and differentiation (18, 44–46). PPARγ plays a pivotal role in the progression of liver fibrosis since HSC activation is associated with a reduction in both expression and transcriptional activity of this nuclear receptor (26, 27). In culture-activated HSCs, synthetic PPARγ ligands restore PPARγ and reverse the activated HSCs to the quiescent phenotype (26–28). In vivo, the administration of synthetic PPARγ ligands (i.e., antidiabetic thiazolidinediones) to animal models of liver fibrosis effectively reduces HSC

transdifferentiation and collagen deposition (47). Furthermore, the results obtained in our trans-activation reporter assay are indicative that SC-236 not only restores PPARγ expression but also works as a PPARγ ligand. This effect was very potent and comparable with the induction exerted by 15d-PGJ_2, the natural ligand and activator of PPARγ. This feature appears to be not exclusive of SC-236 since similar actions have recently been described with other structurally related selective COX-2 inhibitors (21, 48). These findings, together with the observation that the anti-proliferative effects of SC-236 were similar to those exerted by the PPARγ ligand rosiglitazone, support the concept that the anti-fibrotic properties of SC-236 are mediated, at least in part, by PPARγ activation.

Our results indicate that 15d-PGJ_2 is generated in vivo in rat livers and that hepatic 15d-PGJ_2 levels are dramatically increased in CCl_4-treated rats. 15d-PGJ_2 is a downstream metabolite produced by dehydration of PGD_2 (49), which is formed abundantly in the liver and is considered the major hepatic COX product (25). Apparently, in vivo, the dominant source of 15d-PGJ_2 formation is COX-2 (50). Indeed, in our study the increased hepatic 15d-PGJ_2 production in CCl_4-treated rats was significantly abrogated by the selective COX-2 inhibitor, SC-236, confirming that this PG metabolite is predominantly generated via COX-2. In the liver, COX-2-derived 15d-PGJ_2 has been shown to enhance allyl alcohol-induced hepatocyte death (51), thus, inhibition of this non-enzymatic product of PGD_2 by SC-236 may confer further hepato-protection. It is important to note that despite 15d-PGJ_2 is a natural ligand of PPARγ, we observed a discrepancy between the concentrations of 15d-PGJ_2 and the degree of PPARγ expression and activation in the liver of CCl_4-treated rats receiving SC-236, suggesting a 15d-PGJ_2-independent PPARγ activation pathway in this organ.

In summary, the results of the current study bring to light the anti-fibrogenic potential of the selective COX-2 inhibitor SC-236. These drugs are now available for clinical use with a similar efficacy to that of conventional NSAIDs but with lower incidence of adverse gastrointestinal and renal effects (52, 53). Consequently, our results open new avenues for the potential use of selective COX-2 inhibitors as a novel therapy for liver inflammation and fibrosis. Our results also provide new clues on the cellular mechanisms underlying the hepato-protective effects of SC-236, which include inhibition of hepatic MMP-2 and 9 activities and α-SMA levels as well as stimulation of PPARγ and induction of apoptosis in HSCs (Fig. 9). SC-236 also promotes apoptosis in Kupffer cells, which is believed to result in a diminished release of pro-inflammatory mediators (Fig. 9). These mechanisms are probably mediated, at least in part, by the ability of SC-236 to bind and activate PPARγ.

ACKNOWLEDGMENTS

These studies were supported in part by grants from Ministerio de Ciencia y Tecnología (SAF 03/0586) and Instituto de Salud Carlos III (C03/02). A. P. and E. T. were supported by IDIBAPS and M. L.-P. by Ministerio de Ciencia y Tecnología. We thank R. Evans (Salk Institute, La Jolla, USA) for the kind gift of the constructs needed for PPARγ trans-activation studies and R. Bataller and P. Sancho-Bru for expert assistance in the isolation of rat hepatic stellate cells.

REFERENCES

1. Friedman, S. L. (2004) Mechanisms of hepatic fibrosis and therapeutic implications. *Nature Clinical Practice in Gastroenterology and Hepatology* **1,** 98–105

2. Brenner, D. A., Waterboer, T., Choi, S. K., Linquist, J. N., Stefanovic, B., Burchardt, E., Yamauchi, M., Guillan, A., and Rippe, R. A. (2000) New aspects of hepatic fibrosis. *J. Hepatol.* **32,** 32–38

3. Tome, S., and Lucey, M. R. (2004) Review article: current management of alcoholic liver disease. *Aliment. Pharmacol. Ther.* **19,** 707–714

4. Endoh, T., Tang, Q., Denda, A., Noguchi, O., Kobayashi, E., Tamura, K., Horiguchi, K., Ogasawara, H., Tsujiuchi, T., Nakae, D., et al. (1996) Inhibition by acetylsalicylic acid, a cyclo-oxygenase inhibitor, and p-bromophenacylbromide, a phospholipase A2 inhibitor, of both cirrhosis and enzyme-altered nodules caused by a choline-deficient, L-amino acid-defined diet in rats. *Carcinogenesis* **17,** 467–475

5. Clària, J., and Arroyo, V. (2003) Prostaglandins and other cyclooxygenase-dependent arachidonic acid metabolites and the kidney in liver disease. *Prostaglandins Other Lipid Mediat.* **72,** 19–33

6. Vane, J. R., Bakhle, Y. S., and Botting, R. M. (1998) Cyclooxygenases 1 and 2. *Annu. Rev. Pharmacol. Toxicol.* **38,** 97–120

7. Clària, J. (2003) Cyclooxygenase-2 biology. *Curr. Pharm. Des.* **9,** 2177–2190

8. Cheng, J., Imanishi, H., Iijima, H., Shimomura, S., Yamamoto, T., Amuro, Y., Kubota, A., and Hada, T. (2002) Expression of cyclooxygenase 2 and cytosolic phospholipase A(2) in the liver tissue of patients with chronic hepatitis and liver cirrhosis. *Hepatol. Res.* **23,** 185–195

9. Mohammed, N. A., El Aleem, S. A., El Hafiz, H. A., and McMahon, R. F. (2004) Distribution of constitutive (COX-1) and inducible (COX-2) cyclooxygenase in postviral human liver cirrhosis: a possible role for COX-2 in the pathogenesis of liver cirrhosis. *J. Clin. Pathol.* **57,** 350–354

10. Núñez, O., Fernández-Martínez, A., Majano, P. L., Apolinario, A., Gómez-Gonzalo, M., Benedicto, I., López-Cabrera, M., Boscá, L., Clemente, G., García-Monzón, C., et al. (2004) Increased intrahepatic cyclooxygenase 2, matrix metalloproteinase 2, and matrix metalloproteinase 9 expression is associated with progressive liver disease in chronic hepatitis C virus infection: role of viral core and NS5A proteins. *Gut* **53,** 1665–1672

11. Nanji, A. A., Zakim, D., Rahemtulla, A., Daly, T., Miao, L., Zhao, S., Khwaja, S., Tahan, S. R., and Dannenberg, A. J. (1997) Dietary saturated fatty acids down-regulate cyclooxygenase-2 and tumor necrosis factor alfa and reverse fibrosis in alcohol-induced liver disease in the rat. *Hepatology* **26,** 1538–1545

12. Nanji, A. A., Miao, L., Thomas, P., Rahemtulla, A., Khwaja, S., Zhao, S., Peters, D., Tahan, S. R., and Dannenberg, A. J. (1997) Enhanced cyclooxygenase-2 gene expression in alcoholic liver disease in the rat. *Gastroenterology* **112,** 943–951

13. Yamamoto, H., Kondo, M., Shoji, N., Nagano, H., Wakasa, K. I., Sugita, Y., Chang-De, J., Kobayashi, S., Damdinsuren, B., Dono, K., et al. (2003) JTE-522, a cyclooxygenase-2 inhibitor, is an effective chemopreventive agent against rat experimental liver fibrosis. *Gastroenterology* **125,** 556–571

14. Miyajima, A., Ito, K., Asano, T., Seta, K., Ueda, A., and Hayakawa, M. (2001) Does cyclooxygenase-2 inhibitor prevent renal tissue damage in unilateral ureteral obstruction? *J. Urol.* **166,** 1124–1129

15. Frungieri, M. B., Weidinger, S., Meineke, V., Kohn, F. M., and Mayerhofer, A. (2002) Proliferative action of mast-cell tryptase is mediated by PAR2, COX2, prostaglandins, and PPARgamma: Possible relevance to human fibrotic disorders. *Proc. Natl. Acad. Sci. USA* **99,** 15072–15077

16. Tsai, C. H., Chou, M. Y., and Chang, Y. C. (2003) The up-regulation of cyclooxygenase-2 expression in human buccal mucosal fibroblasts by arecoline: a possible role in the pathogenesis of oral submucous fibrosis. *J. Oral Pathol. Med.* **32,** 146–153

17. Deulofeu, R., Parés, A., Rubio, M., Gassó, M., Roman, J., Giménez, A., Varela-Moreiras, G., Caballeria, J., Ballesta, A. M., Mato, J. M., et al. (2000) S-adenosylmethionine prevents hepatic tocopherol depletion in carbon tetrachloride-injured rats. *Clin. Sci.* **99,** 315–320

18. Forman, B. M., Tontonoz, P., Chen, J., Brun, R. P., Spiegelman, B. M., and Evans, R. M. (1995) 15-Deoxy-delta 12, 14-prostaglandin J_2 is a ligand for the adipocyte determination factor PPAR gamma. *Cell* **83,** 803–812

19. Bligh, E. G., and Dyer, W. J. (1959) A rapid method of total lipid extraction and purification. *Can. J. Med. Sci.* **37,** 911–917

20. Titos, E., Clària, J., Planagumà, A., López-Parra, M., Villamor, N., Párrizas, M., Carrió, A., Miquel, R., Jiménez, W., Arroyo, V., et al. (2003) Inhibition of 5-lipoxygenase induces cell growth arrest and apoptosis in rat Kupffer cells: implications for liver fibrosis. *FASEB J.* **17,** 1745–1747

21. Planagumà, A., Titos, E., López-Parra, M., Gaya, J., Pueyo, G., Arroyo, V., and Clària, J. (2002) Aspirin (ASA) regulates 5-lipoxygenase activity and peroxisome proliferator-activated receptor alpha-mediated CINC-1 release in rat liver cells: novel actions of lipoxin A_4 (LXA_4) and ASA-triggered 15-epi-LXA_4. *FASEB J.* **16,** 1937–1939

22. Bataller, R., Gasull, X., Ginès, P., Hellemans, K., Gorbig, M. N., Nicolas, J. M., Sancho-Bru, P., De Las Heras, D., Gual, A., Geerts, A., et al. (2001) In vitro and in vivo activation of rat hepatic stellate cells results in de novo expression of L-type voltage-operated calcium channels. *Hepatology* **33,** 956–962

23. Benyon, R. C., and Arthur, M. J. (2001) Extracellular matrix degradation and the role of hepatic stellate cells. *Semin. Liver Dis.* **21,** 373–384

24. Enomoto, N., Ikejima, K., Yamashina, S., Enomoto, A., Nishiura, T., Nishimura, T., Brenner, D. A., Schemmer, P., Bradford, B. U., Rivera, C. A., et al. (2000) Kupffer cell-derived prostaglandin E(2) is involved in alcohol-induced fat accumulation in rat liver. *Am. J. Physiol. Gastrointest. Liver Physiol.* **279,** G100–G106

25. Decker, K. (1990) Biologically active products of stimulated liver macrophages (Kupffer cells). *Eur. J. Biochem.* **192,** 245–261

26. Marra, F., Efsen, E., Romanelli, R. G., Caligiuri, A., Pastacaldi, S., Batignani, G., Bonacchi, A., Caporale, R., Laffi, G., Pinzani, M., et al. (2000) Ligands of peroxisome proliferator-activated receptor gamma modulate profibrogenic and proinflammatory actions in hepatic stellate cells. *Gastroenterology* **119,** 466–478

27. Miyahara, T., Schrum, L., Rippe, R., Xiong, S., Yee, H. F., Jr., Motomura, K., Anania, F. A., Willson, T. M., and Tsukamoto, H. (2000) Peroxisome proliferator-activated receptors and hepatic stellate cell activation. *J. Biol. Chem.* **275,** 35715–35722

28. Hazra, S., Xiong, S., Wang, J., Rippe, R. A., Chatterjee, K. K., and Tsukamoto, H. (2004) Peroxisome proliferator-activated receptor γ induces a phenotypic switch from activated to quiescent hepatic stellate cells. *J. Biol. Chem.* **279,** 11392–11401

29. Lehman, J. M., Lenhard, J. M., Oliver, B. B., Ringold, G. M., and Kliewer, S. A. (1997) Peroxisome proliferator-activated receptors α and γ are activated by indomethacin and other non-steroidal anti-inflammatory drugs. *J. Biol. Chem.* **272,** 3406–3410

30. Souto, E. O., Miyoshi, H., Dubois, R. N., and Gores, G. J. (2001) Kupffer cell-derived cyclooxygenase-2 regulates hepatocyte Bcl-2 expression in choledocho-venous fistula rats. *Am. J. Physiol. Gastrointest. Liver Physiol.* **280,** G805–G811

31. Efsen, E., Bonacchi, A., Pastacaldi, S., Valente, A. J., Wenzel, U. O., Tosti-Guerra, C., Pinzani, M., Laffi, G., Abboud, H. E., Gentilini, P., et al. (2001) Agonist-specific regulation of monocyte chemoattractant protein-1 expression by cyclooxygenase metabolites in hepatic stellate cells. *Hepatology* **33,** 713–721

32. Gallois, C., Habib, A., Tao, J., Moulin, S., Maclouf, J., Mallat, A., and Lotersztajn, S. (1998) Role of NF-kappaB in the antiproliferative effect of endothelin-1 and tumor necrosis factor-alpha in human hepatic stellate cells. Involvement of cyclooxygenase-2. *J. Biol. Chem.* **273,** 23183–23190

33. Hui, A. Y., Dannenberg, A. J., Sung, J. J. Y., Subbaramaiah, K., Du, B., Olinga, P., and Friedman, S. L. (2004) Prostaglandin E_2 inhibits transforming growth factor beta 1-mediated induction of collagen alpha 1(I) in hepatic stellate cells. *J. Hepatol.* **41,** 251–258

34. Jiang, X. H., Lam, S. K., Lin, M. C., Jiang, S. H., Kung, H. F., Slosberg, E. D., Soh, J. W., Weinstein, I. B., and Wong, B. C. (2002) Novel target for induction of apoptosis by cyclo-

oxygenase-2 inhibitor SC-236 through a protein kinase C-beta(1)-dependent pathway. *Oncogene* **21,** 6113–6122

35. Romano, M., and Clària, J. (2003) Cyclooxygenase-2 and 5-lipoxygenase converging functions on cell proliferation and tumor angiogenesis: implications for cancer therapy. *FASEB J.* **17,** 1986–1995

36. Iredale, J. P., Benyon, R. C., McCullen, P. M., Northrop, M., Pawley, S., Hovell, C., and Arthur, M. J. P. (1998) Mechanisms of spontaneous resolution of rat liver fibrosis. *J. Clin. Invest.* **102,** 538–549

37. Wright, M. C., Issa, R., Smart, D. E., Trim, N., Murray, G. I., Primrose, J. N., Arthur, M. J. P., Iredale, J. P., and Mann, D. A. (2001) Gliotoxin stimulates the apoptosis of human and rat hepatic stellate cells and enhances the resolution of liver fibrosis in rats. *Gastroenterology* **121,** 685–698

38. Friedman, S. L. (2005) Mac the knife? Macrophages-the double-edged sword of hepatic fibrosis. *J. Clin. Invest.* **115,** 29–32

39. Geerts, A., Schellinck, P., Bouwens, L., and Wisse, E. (1988) Cell population kinetics of Kupffer cells during the onset of fibrosis in rat liver by chronic carbon tetrachloride administration. *J. Hepatol.* **6,** 50–56

40. Duffield, J. S., Forbes, S. J., Constandinou, C. M., Clay, S., Partolina, M., Vuthoori, S., Wu, S., Lang, R., and Iredale, J. P. (2005) Selective depletion of macrophages reveals distinct, opposing roles during liver injury and repair. *J. Clin. Invest.* **115,** 56–65

41. Badawi, A. F., Eldeen, M. B., Liu, Y., Ross, E. A., and Badr, M. Z. (2004) Inhibition of rat mammary gland carcinogenesis by simultaneous targeting of cyclooxygenase-2 and peroxisome proliferator-activated receptor gamma. *Cancer Res.* **64,** 1181–1189

42. Wong, B. C., Jiang, X. H., Lin, M. C., Tu, S. P., Cui, J. T., Jiang, S. H., Wong, W. M., Yuen, M. F., Lam, S. K., and Kung, H. F. (2004) Cyclooxygenase-2 inhibitor (SC-236) suppresses activator protein-1 through c-Jun NH2-terminal kinase. *Gastroenterology* **126,** 136–147

43. Leng, J., Han, C., Demetris, A. J., Michalopoulos, G. K., and Wu, T. (2003) Cyclooxygenase-2 promotes hepatocellular carcinoma cell growth through Akt activation: evidence for Akt inhibition in celecoxib-induced apoptosis. *Hepatology* **38,** 756–768

44. Negishi, M., and Katoh, H. C. (2002) Cyclopentenone prostaglandin receptors. *Prostaglandins Other Lipid Mediat.* **68-69,** 611–617

45. Ricote, M., Li, A. C., Willson, T. M., Kelly, C. J., and Glass, C. K. (1998) The peroxisome proliferator-activated receptor-gamma is a negative regulator of macrophage activation. *Nature* **391,** 79–82

46. Jiang, C., Ting, A. T., and Seed, B. (1998) PPAR-gamma agonists inhibit production of monocyte inflammatory cytokines. *Nature* **391,** 82–86

47. Galli, A., Crabb, D. W., Ceni, E., Salzano, R., Mello, T., Svegliati-Baroni, G., Ridolfi, F., Trozzi, L., Surrenti, C., and Casini, A. (2002) Antidiabetic thiazolidinediones inhibit collagen synthesis and hepatic stellate cell activation in vivo and in vitro. *Gastroenterology* **122,** 1924–1940

48. López-Parra, M., Clària, J., Titos, E., Planagumà, A., Párrizas, M., Masferrer, J. L., Jiménez, W., Arroyo, V., Rivera, F., and Rodés, J. (2005) The selective cyclooxygenase-2 inhibitor celecoxib modulates the formation of vasoconstrictor eicosanoids and activates PPARgamma. Influence of albumin. *J. Hepatol.* **42,** 75–81

49. Kikawa, Y., Narumiya, S., Fukushima, M., Wakatsuka, H., and Hayaishi, O. (1984) 9-Deoxy-delta 9, delta 12-13,14-dihydroprostaglandin D_2, a metabolite of prostaglandin D_2 formed in human plasma. *Proc. Natl. Acad. Sci. USA* **81,** 1317–1321

50. Bell-Parikh, L. C., Ide, T., Lawson, J. A., McNamara, P., Reilly, M., and FitzGerald, G. A. (2003) Biosynthesis of 15-deoxy-delta12,14-PGJ_2 and the ligation of PPARgamma. *J. Clin. Invest.* **112,** 945–955

51. Maddox, J. F., Domsalski, A. C., Roth, R. A., and Ganey, P. E. (2004) 15-deoxy prostaglandin J_2 enhances allyl alcohol-induced toxicity in rat hepatocytes. *Toxicol. Sci.* **77,** 290–298

52. Bosch-Marcé, M., Clària, J., Titos, E., Masferrer, J. L., Altuna, R., Poo, J. L., Jiménez, W., Arroyo, V., Rivera, F., and Rodés, J. (1999) Selective inhibition of cyclooxygenase 2 spares renal function and prostaglandin synthesis in cirrhotic rats with ascites. *Gastroenterology* **116,** 1167–1175

53. López-Parra, M., Clària, J., Planagumà, A., Titos, E., Masferrer, J. L., Woerner, B. M., Koki, A. T., Jiménez, W., Altuna, R., Arroyo, V., et al. (2002) Cyclooxygenase-1 derived prostaglandins are involved in the maintenance of renal function in rats with cirrhosis and ascites. *Br. J. Pharmacol.* **135,** 891–900

Received August 20, 2004; accepted March 14, 2005.

Table 1

Histological assessment of the degree of liver fibrosis in CCl_4-treated rats receiving either placebo or SC-236.

	Weeks of CCl_4 treatment		
	6	**8**	**10**
STUDY A			
Placebo (*n*=30)	0.80 ± 0.29	1.90 ± 0.31	3.10 ± 0.24
SC-236 (*n*=30)	0.80 ± 0.31	2.20 ± 0.20	2.40 ± 0.36
***P*-value**	NS	NS	<0.05
STUDY B			
Placebo (*n*=6)	2.50 ± 0.50	4.00 ± 0.00	3.50 ± 0.50
SC-236 (*n*=10)	0.00 ± 0.00	2.00 ± 0.58	2.25 ± 0.25
***P*-value**	<0.05	<0.05	NS

CCl_4-treated rats were randomly assigned to receive either placebo (0.5 % carboxymethylcellulose) or SC-236 (6 mg/kg b.w., p.o.) and dosed weekly (Study A) or three times per week (Study B), starting one week before the first administration of CCl_4. Animals were sacrificed in a staggered fashion at the 6^{th}, 8^{th}, and 10^{th} week of the CCl_4 induction program and liver sections histologically analyzed and scored according to the parameters established under Material and Methods. Data are expressed as mean ± SEM.

Table 2

Hepatic hydroxyproline concentrations in CCl_4-treated rats receiving either placebo or SC-236.

	Weeks of CCl_4 treatment		
	6	**8**	**10**
STUDY A			
Placebo (*n*=30)	12.7 ± 1.5	16.9 ± 1.4	18.6 ± 1.4
SC-236 (*n*=30)	11.5 ± 1.6	13.0 ± 1.4	21.1 ± 2.1
***P*-value**	NS	<0.05	NS
STUDY B			
Placebo (*n*=6)	7.0 ± 0.6	18.8 ± 3.2	16.9 ± 4.3
SC-236 (*n*=10)	10.4 ± 0.5	10.3 ± 0.8	10.6 ± 2.3
***P*-value**	NS	<0.05	NS

CCl_4-treated rats were randomly assigned to receive either placebo (0.5 % carboxymethylcellulose) or SC-236 (6 mg/kg b.w., p.o.) and dosed weekly (Study A) or three times per week (Study B), starting one week before the first administration of CCl_4. Animals were sacrificed in a staggered fashion at the 6^{th}, 8^{th}, and 10^{th} week of the CCl_4 induction program and hydroxyproline levels determined as described in Material and Methods. Hydroxyproline levels are given in nmol/mg liver tissue and expressed as mean ± SEM.

Fig. 1

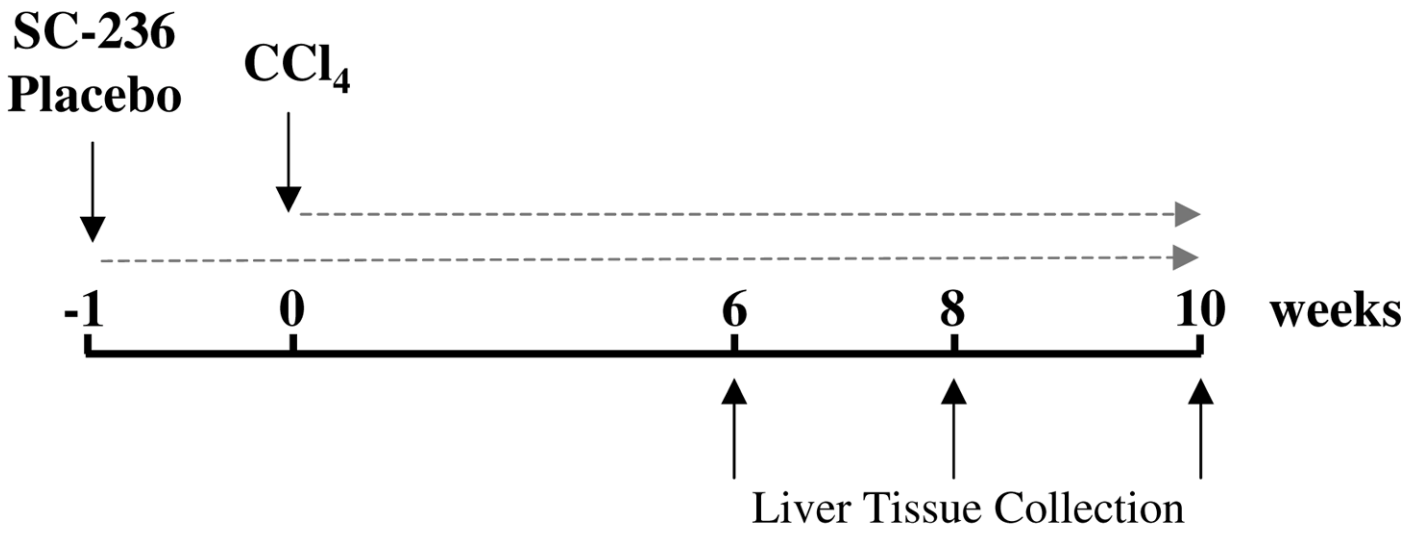

Figure 1. Schematic diagram of the experimental design for Study A. Sixty male adult Wistar rats were submitted to the fibrosis induction protocol by inhalation of CCl_4. These animals were divided into two groups, which received either the selective COX-2 inhibitor SC-236 (6 mg/kg b.w., p.o.) or placebo (0.5% carboxymethylcellulose), starting one week before the first administration of CCl_4. After 6, 8, and 10 weeks of CCl_4 treatment, the animals were sacrificed in a staggered fashion and liver tissue samples were collected for further analysis.

Fig. 2

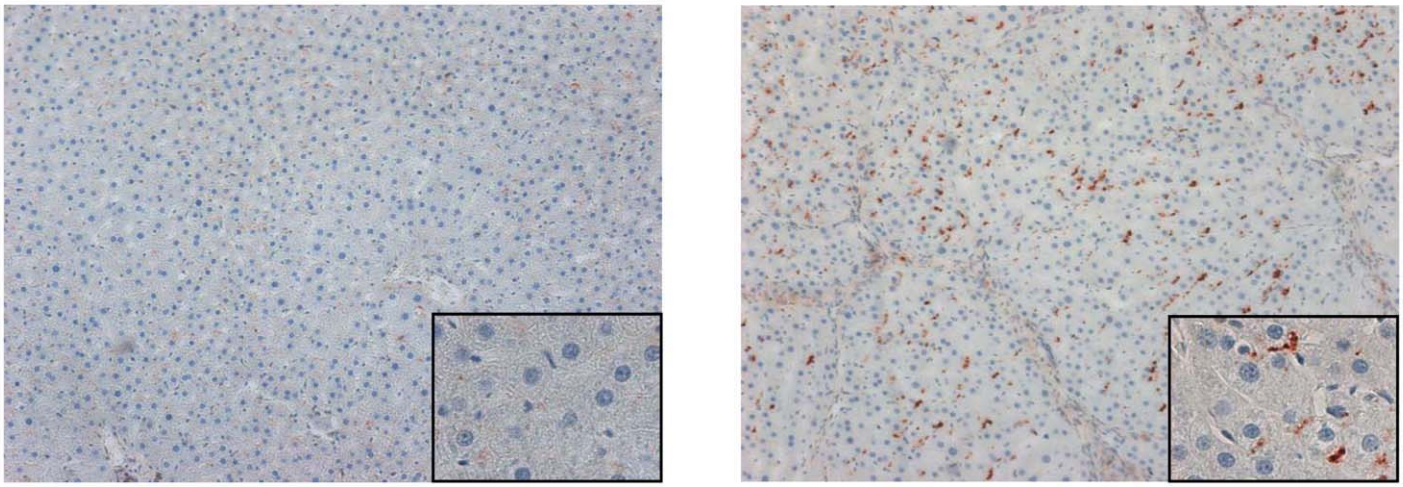

Figure 2. Immunohistochemical analysis of COX-2 protein expression in livers from control and CCl_4-treated rats. Liver samples from control and CCl_4-treated rats (10 weeks) were fixed with MBF, embedded in paraffin, sectioned at 5 µm onto glass slides, and incubated with a polyclonal rabbit anti-murine COX-2 serum. Positive COX-2 staining was visualized with the peroxidase substrate AEC. (Original magnification: ×100; *inset*: ×400).

Fig. 3

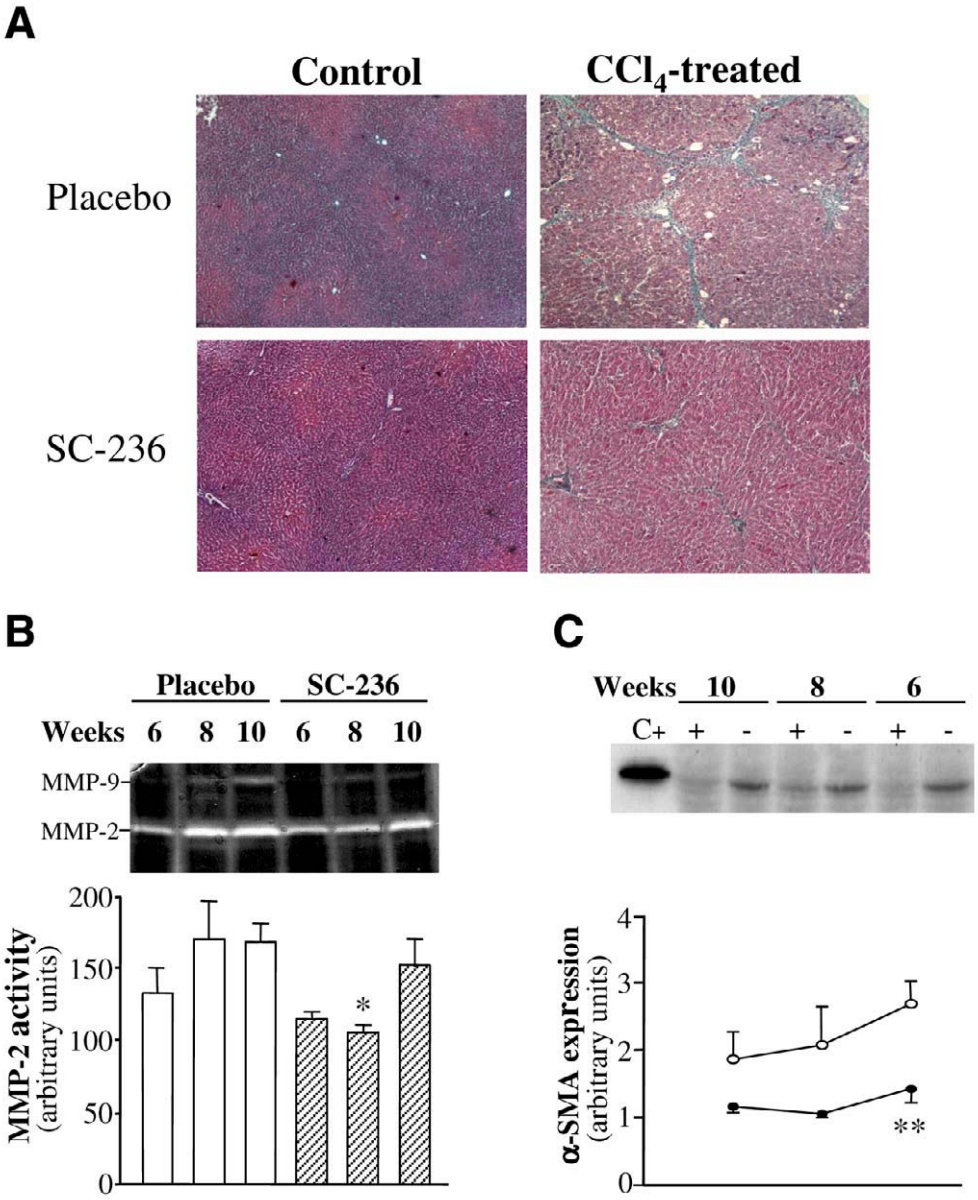

Figure 3. Anti-fibrotic effects of SC-236 in CCl_4-treated rats. ***A*)** Histological assessment of liver fibrosis in CCl_4-treated and control rats. The extent of matrix deposition was measured by Masson´s trichrome staining of liver tissue sections from control animals (***left panels***) (magnification ×40) and 10-week CCl_4-treated rats (***right panels***) (magnification ×100) receiving either placebo (***upper panels***) or SC-236 (***lower panels***). These data are representative of results obtained from 10 control and 20 CCl_4-treated rats. ***B*)** Detection of hepatic MMP-2 and MMP-9 activities by zymography. Gelatin polyacrilamide gel representative of changes in activity of MMP-2 (72 kDa) and MMP-9 (92 kDa) along the weeks of CCl_4 administration (6, 8, and 10 weeks) in CCl_4-treated rats receiving placebo or SC-236. The lower panel shows the analysis by densitometry of MMP-2 activity in these samples. The results are the mean ± SEM of five different experiments. $*P <$ 0.05 versus placebo. ***C*)** Effects of SC-236 on hepatic α-SMA protein expression in CCl_4-treated rats. Liver tissue samples from rats with CCl_4-induced fibrosis treated with (+) or without (–) SC-236 were analyzed by Western blot using a specific antibody against α-SMA. A representative blot is shown in the upper panel whereas the histogram in the ***lower panel*** shows the results obtained from the densitometric analysis of band intensities from four separate experiments (mean ± SEM). (○) placebo, (●) SC-236. CT+, total protein from mesangial cells. $**P < 0.01$ versus placebo.

Fig. 4

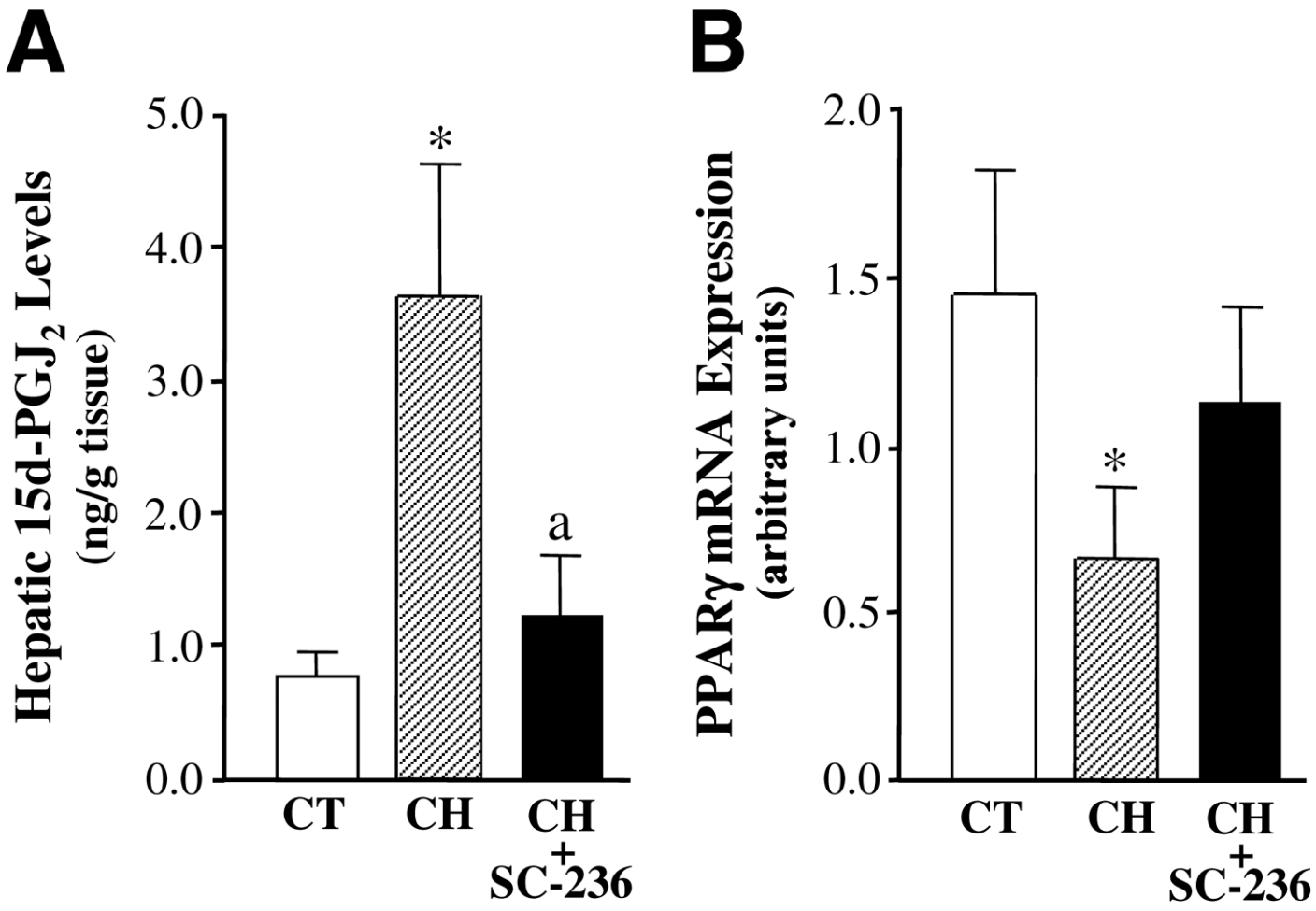

Figure 4. ***A*)** Hepatic levels of 15d-PGJ_2 in control (CT, *n*=5) and CCl_4-treated rats receiving placebo (CH, *n*=10), or SC-236 (CH+SC-236, *n*=10). Liver tissue samples from control and 8-week CCl_4-treated rats were homogenized, extracted in C_{18}-silica reverse-phase cartridges, and 15d-PGJ_2 levels determined by a highly specific EIA. Results are expressed as mean ± SEM with duplicate determinations. **P* < 0.01 versus CT group; a, *P* < 0.025 versus CH group. ***B*)** PPARγ mRNA expression was determined by reverse-transcription real-time quantitative PCR in liver tissue from the three groups of animals (CT, CH, and CH+SC-236). Results are expressed as mean ± SEM with duplicate determinations. **P* < 0.05 versus CT group.

Fig. 5

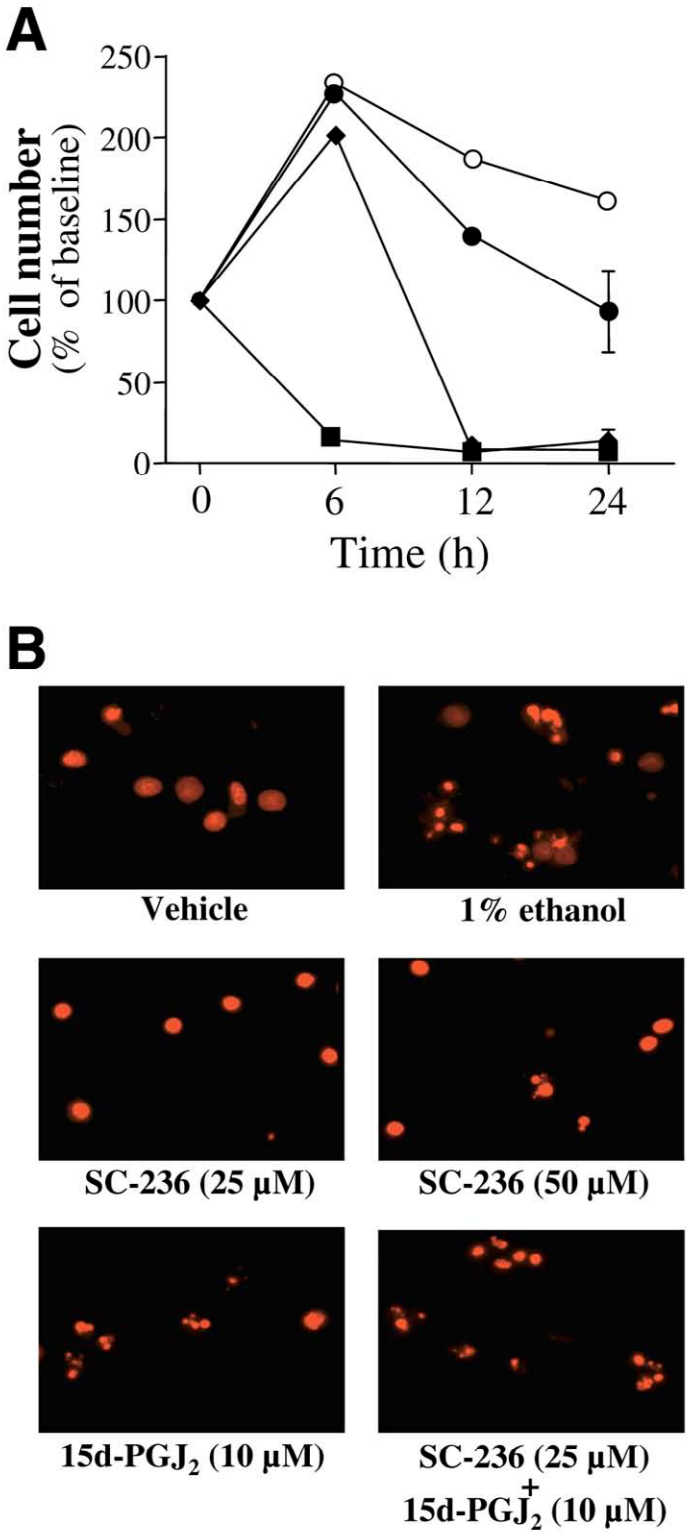

Figure 5. Effects of SC-236 on Kupffer cell number and survival. ***A*)** Cell number was evaluated by the MTT assay as described in Material and Methods. Rat macrophages were treated with vehicle (0.5% ethanol) (○) and increasing concentrations of SC-236 (10 (●), 15 (◆), and 25 (■) µM) for 0, 6, 12, and 24 h at 37ºC. Cell number was expressed as percentage (%) with respect to baseline. ***B*)** Apoptotic changes in nuclear morphology were assessed by fluorescence microscopy in Kupffer cells stained with propidium iodide after incubation with vehicle (0.1% ethanol), 1% ethanol, SC-236 (25 and 50 µM), 15d-PGJ_2 (10 µM) alone, or in combination with SC-236 (25 µM) for 6 h at 37ºC.

Fig. 6

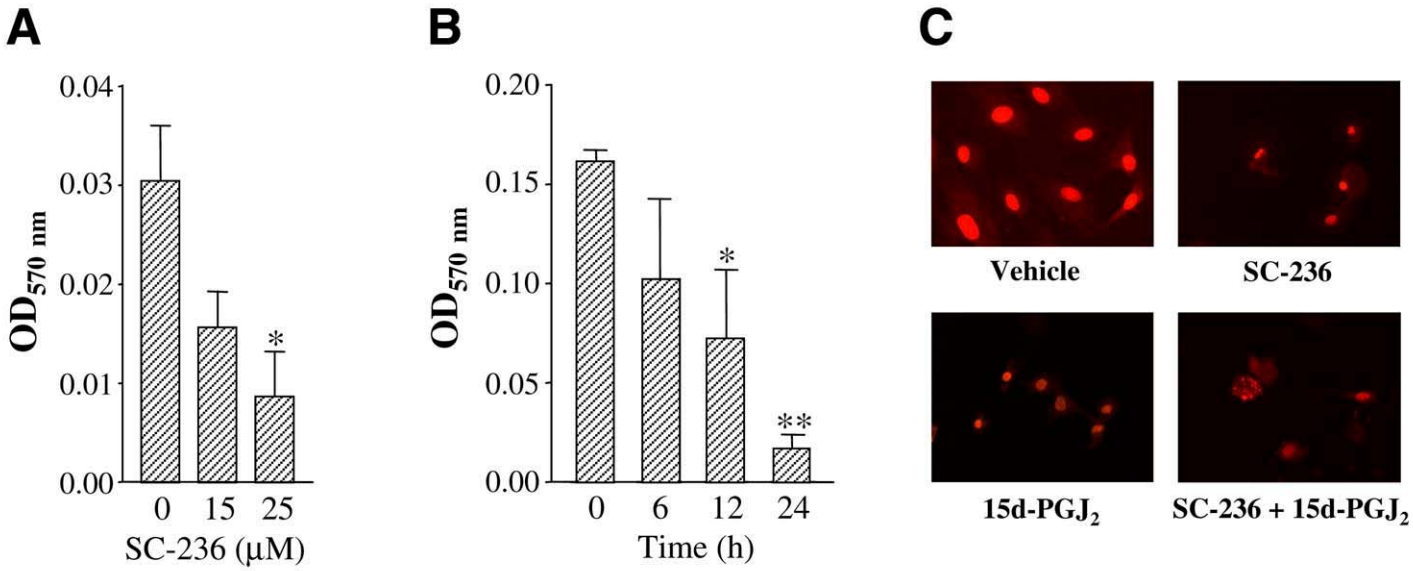

Figure 6. Effects of SC-236 on HSC growth and survival. Concentration- and time-responses to SC-236. HSCs were incubated with increasing concentrations of SC-236 (0, 15, and 25 μM) for 24 h (***A***) or grown for 0, 6, 12, and 24 h with 15 μM SC-236 (***B***), and cell number was determined by the MTT assay. Results are the mean ± SEM of three different experiments with duplicate determinations. *$P < 0.05$ and **$P < 0.01$ versus untreated cells. ***C***) Changes in nuclear morphology associated with programmed cell death were assessed by fluorescence microscopy in HSCs stained with propidium iodide after 6 h of incubation at 37ºC with vehicle (0.1% ethanol), SC-236 (25 μM), and 15d-PGJ_2 (10 μM) alone or in combination with SC-236 (25 μM).

Fig. 7

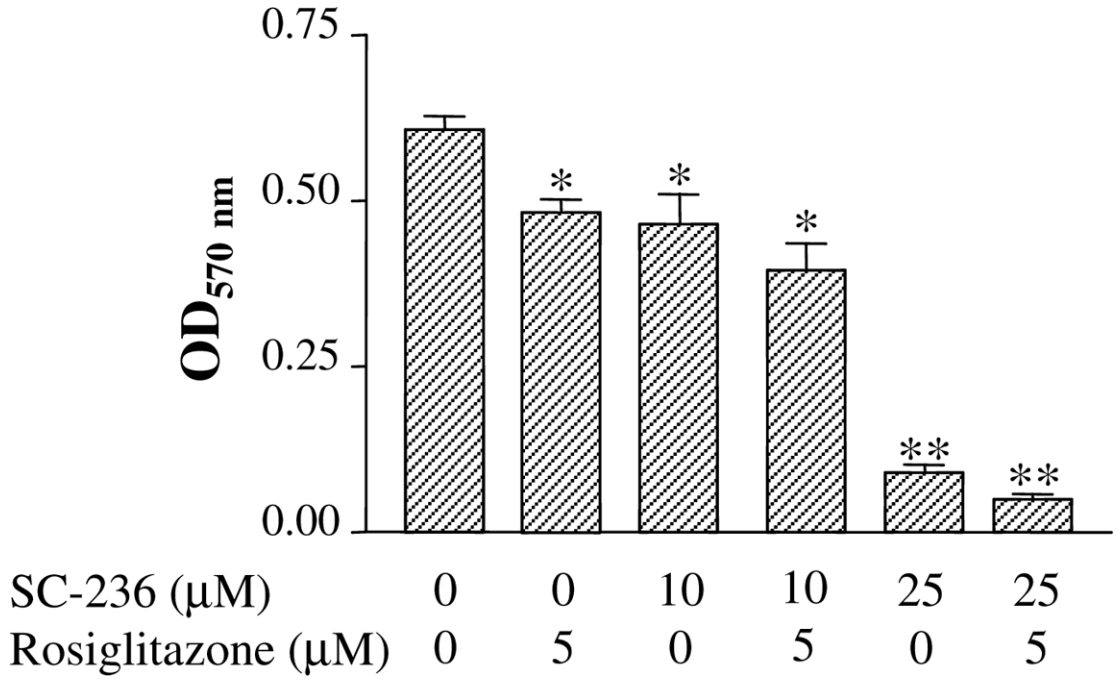

Figure 7. Comparison of the effects of SC-236 and rosiglitazone on HSC proliferation. Serum-starved HSCs were pre-incubated with SC-236 (10 and 25 μM) and rosiglitazone (5 μM) for 15 min before exposure to PDGF (10 ng/ml) for 18 h at 37ºC. HSC number was evaluated by the MTT assay as described in Materials and Methods. Results are the mean ± SEM of three different experiments with duplicate determinations. *$P < 0.05$ and **$P < 0.01$ versus untreated cells.

Fig. 8

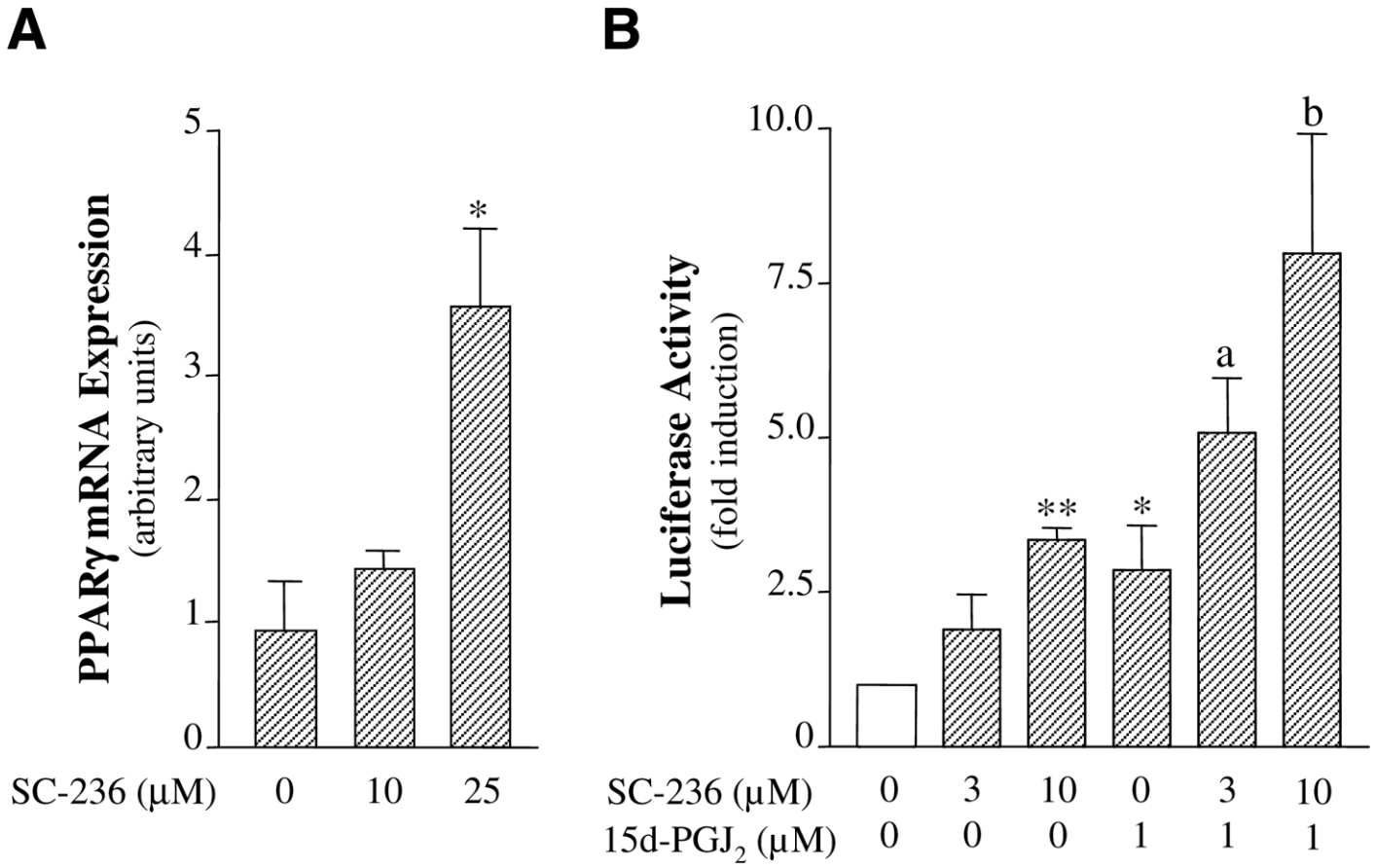

Figure 8. Effects of SC-236 on PPARγ mRNA expression and PPARγ activity. ***A***) HSCs were exposed to increasing concentrations of SC-236 (0, 10, and 25 μM) for 6 h at 37°C and PPARγ mRNA expression was measured by reverse transcription real-time quantitative PCR. Results are the mean ± SEM of three different experiments with duplicate determinations. **P* < 0.05 versus untreated cells. ***B***) The binding and activation of PPARγ by SC-236 was assessed in a cell-based luciferase reporter transactivation assay after an incubation of 18 h with increasing concentrations of SC-236 (3 and 10 μM) alone or in combination with 15d-PGJ_2 (1 μM). Luciferase activity was normalized to the level of β-gal activity and results expressed as fold induction relative to untreated cells. Results are the mean ± SEM of four different experiments with duplicate determinations. **P* < 0.05 and ***P* < 0.001 versus vehicle. a, *P* < 0.05 and b, *P* < 0.025 versus 15d-PGJ_2 alone.

Fig. 9

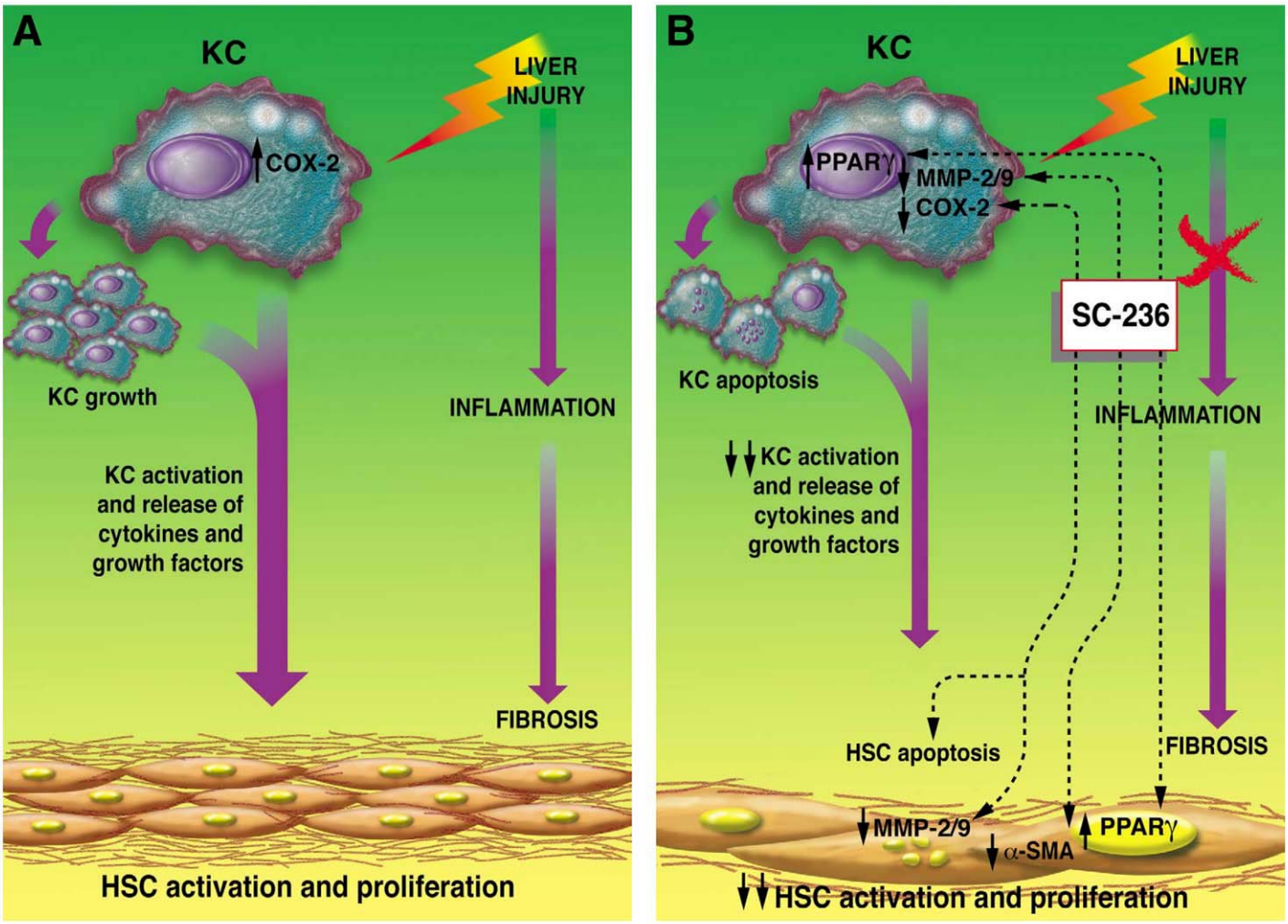

Figure 9. Summary of the proposed mechanism by which SC-236 attenuates liver fibrosis. ***A*)** Liver injury induces COX-2 over-expression in Kupffer cells (KC) and initiates a cascade of events, including the massive production of cytokines and growth factors, leading to hepatic stellate cell (HSC) activation and proliferation and consequently to liver fibrosis. In addition, during fibrosis progression, KC proliferate, thereby amplifying the release of pro-inflammatory mediators. ***B*)** The selective COX-2 inhibitor dampens liver inflammation and fibrosis by mechanisms involving PPARγ activation, down-regulation of α-SMA expression, and MMP-2 and -9 activities and induction of KC and HSC apoptosis.